The Effect of Multicomponent Diffusion on the Chemical Composition of Seawater

by

Nikolaos Simantiris

B.Sc., University of the Aegean, 2016

A THESIS SUBMITTED IN PARTIAL FULFILLMENT
OF THE REQUIREMENTS FOR THE DEGREE OF

Master of Science

in

THE FACULTY OF GRADUATE AND POSTDOCTORAL STUDIES
(Oceanography)

The University of British Columbia
(Vancouver)

October 2019

The following individuals certify that they have read, and recommend to the Faculty of Graduate and Postdoctoral Studies for acceptance, the thesis entitled:

The Effect of Multicomponent Diffusion on the Chemical Composition of Seawater

submitted by **Nikolaos Simantiris** in partial fulfillment of the requirements for the degree of **Master of Science** in **Oceanography**.

Examining Committee:

Richard Pawlowicz, Physical Oceanographer
Supervisor

Ulrich Mayer, Hydrologist
Supervisory Committee Member

Greg Lawrence, Hydrotechnical Engineer
Supervisory Committee Member

Abstract

Double-diffusive convection or Double Diffusion is an interaction within a fluid whose density is governed by two constituents of different molecular diffusivities. Double diffusion in the ocean appears to create unique structures that look like staircases in vertical profiles of temperature and salinity. Many oceanographers believe that double diffusion can affect the water masses and the circulation of the ocean. However, in the current literature the detailed physics behind the formation of this staircase are still unclear. In sea salt each ion has different diffusion rate and because of that modelling salt diffusion is actually more complicated since there is no single ”salt diffusivity”. Therefore in order to describe the effects of double diffusion in seawater we have to consider a multicomponent system where each ion is reacting differently than the other ones. To simulate this system we use MIN3P a multicomponent diffusion model. Our approach is primarily numerical, but in order to test the conclusions of our model we compare against observations in Powell Lake. We see that Multicomponent Diffusion can change the chemical composition of seawater and should be considered an important transport mechanism in the ocean.

Lay Summary

The chemical composition of seawater, expressed in ratios between the ions that form the salt content of the ocean, is considered to be similar everywhere in the ocean. Our research shows that in regions where the dominant transport mechanisms that control the ocean are not present, multicomponent diffusion will change the chemical composition of seawater with time. Therefore it should be taken into account when researchers are interested in the chemistry of water samples from these regions.

Preface

This thesis is authored by me, Nikolaos Simantiris, and describes original work carried out by me under the supervision of Dr. Richard Pawlowicz. The setup for the model used for this study was jointly developed with Dr. Richard Pawlowicz and Dr. Ulrich Mayer. Results are unpublished, but are undergoing preparation for submission.

Contents

List of Tables

List of Figures

Acknowledgments

I would like to express my sincere gratitude to all those who stood by me these past 2 years. It was through their help that I was able to finish my thesis and master's degree.

I would like to specifically thank my supervisor Rich Pawlowicz for his endless patience, guidance and effort, helping me become a better scientist and a better person.

I would like to thank the Greek Orthodox Community of Vancouver and especially Fr. Constantinos Economos for his love and tremendous help with my life in Canada.

I would also like to thank my parents, Efstratios and Maria, for their love, support and faith in me. I would have never been able to achieve anything without your help.

And always, both first and last, I would like to thank God. All of my accomplishments are a product of His love and mercy.

Dedication

To Kyriakos

Chapter 1

Introduction

The major ion composition of seawater is believed to be similar everywhere in the ocean (Marcet, 1819; Horne, 1969; Thurman and Burton, 1997; Kennish, 2000; Millero, 2016). This is based on measurements of the chemical composition on seawater samples in various regions of the ocean, and the fact that turbulent mixing is the dominant mechanism that homogenizes the ocean. But, there are some areas that may not be dominated by turbulent mixing such as the Canada Basin in the Arctic ocean (Timmermans et al., 2003), the Black Sea (Murray et al., 1991) and lakes among others. Instead, diffusive processes, that will act to fractionate seawater, may be important. Therefore, the chemical composition in these areas might differ. However, we do not know how large these changes might be and there are no measurements of the major ion composition in water samples from these regions.

Thus, with this study we will investigate the question of how large are the changes in the chemical composition of seawater, that arise from diffusion processes, and whether these changes should be measurable if we had measurements in these regions. But what are these diffusion processes? In the Canada Basin in the Arctic ocean, vertical profiles of temperature and salinity that look like "staircases" indicate that Double Diffusion appears to be an important process in this area. We also know that in Powell Lake in Canada, we can identify Double Diffusive processes acting on ancient seawater which is trapped in the deep basins of the lake. Therefore, Powell Lake may be a useful analogue to study diffusion processes in

the global ocean.

1.1 Double Diffusive Convection in the Ocean

Double-diffusive convection or Double Diffusion (DD) is an interaction within a fluid whose density is governed by two constituents with different molecular diffusivities (Ruddick and Gargett, 2003). Signatures of double diffusive instabilities that arise from the different diffusivities of temperature and salt are observed in many regions of the ocean, especially in some parts of the Arctic, and in some salt-containing lakes around the world (Carpenter and Timmermans, 2012). In the absence of mechanical mixing, the convective motions that are established through the creation of a double diffusive instability may substantially enhance the vertical transports of heat and salt relative to those which would be supported by molecular diffusion alone.

Two types of instability can occur, known as fingering and diffusive instabilities. Fingering instabilities generally occur when temperature and salinity decrease with depth. Diffusive instabilities occur when temperature and salinity increase with depth. Kelley et al. (2003) estimates the world-wide prevalence for double diffusive convection based on theory and laboratory work to show that high-latitude areas in the ocean are susceptible to diffusive instabilities.

Double diffusion in the ocean appears to create unique structures that look like staircases in vertical profiles of temperature and salinity. Through this characteristic it is easy to identify DD around the world. Oceanic staircases under the Arctic ice were first reported by Padman and Dillon (1989). These structures can cover large horizontal areas, but their importance for the global ocean circulation is still uncertain (Ruddick and Gargett, 2003).

In fig. 1.1 we see an observed staircase (Scheifele, 2013) in which two constituents (temperature and salinity) increase with depth. In this example the height of each step is about 1 m and the thickness of the interface between the steps is about 10 cm. The typical interface thickness in the ocean is between 15 cm (Padman and Dillon, 1989; Carpenter and Timmermans, 2012) and 25 cm (Kelley et al., 2003) and the typical step height in the ocean is between 1.5 m (Carpenter and Timmermans, 2012) and 2 m (Padman and Dillon, 1989; Kelley et al., 2003) but with

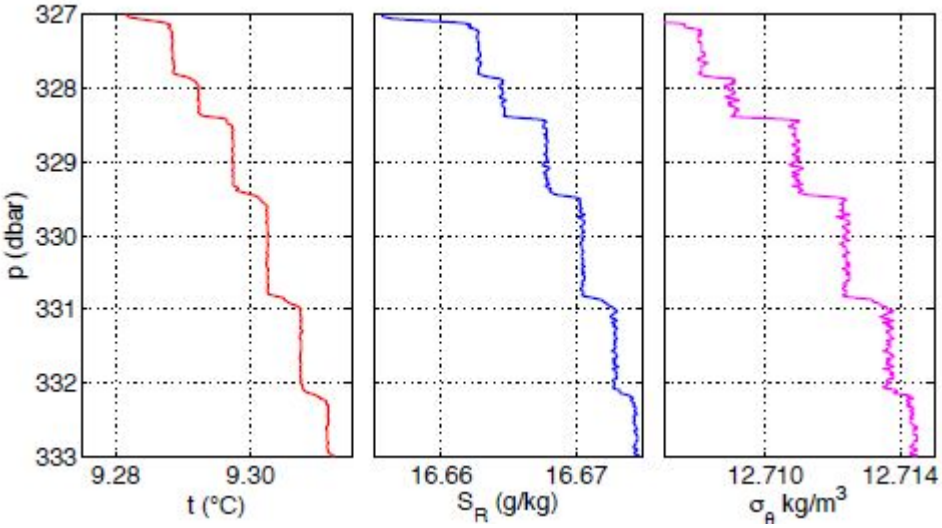

Figure 1.1: An example of double-diffusive layers measured in Powell Lake, B.C., Canada. Shown are in-situ temperature t, Reference Salinity S_R, and potential density (Scheifele, 2013).

exceptions such as the Canada Basin where the step height could be up to 50 m (Timmermans et al., 2003). These staircases seem to be weak structures since the density differences between the steps are very small (on the order of 0.002 kg/m^3) but in fact can be quite stable, with steps remaining coherent for years (Zaloga, 2015).

Many oceanographers believe that double diffusion may affect the water masses and the circulation of the ocean. The importance of mixing in control of the ocean heat storage, the thermohaline circulation, climate, carbon dioxide absorption, and pollutant dispersal, makes it necessary to achieve a more complete understanding of oceanic double diffusion and its consequences (Schmitt, 2002).

In the following sections we will be discussing the physics of this characteristic staircase with the possible instabilities leading to this structure. Typically in studies of DD "sea salt" is treated as a substance with a particular diffusivity, but in fact it contains many substances with different diffusivities. What are the consequences of this simplification? In this thesis we will attempt to understand these consequences. But first, we will review DD.

1.2 Physics of Double Diffusion

The density of seawater in some region of specific temperature (T) and salinity (S) can be approximated as a linear function of both parameters:

$$\rho = \rho_o(1 - \alpha\Delta T + \beta\Delta S) \tag{1.1}$$

where ρ_o is a reference density, ΔT the difference between the observed temperature and a reference temperature (in $^\circ C$), ΔS the difference between the observed salinity and a reference salinity (in g/kg), α is the thermal expansion coefficient and β is the haline contraction coefficient, defined as:

$$\alpha = -\frac{1}{\rho_o}\frac{d\rho}{dT} \tag{1.2}$$

$$\beta = \frac{1}{\rho_o}\frac{d\rho}{dS} \tag{1.3}$$

Double diffusive instabilities arise in cases where the profile of one parameter leads to increase in density with depth, but the other one decreases. Thus, we see that there are two ways to set up a stratification that has one stable and one unstable component but a net stratification that is still stable, and these two scenarios lead to two distinct modes of double diffusion (fig. 1.2).

Assuming oceanographic ranges and stable stratification, if T and S both decrease with depth, temperature is the stable component that contributes the dominating density effect while salinity is the unstable component that intends to destabilize the water column. This leads to the salt fingering mode of diffusive instability. The opposite happens if T and S both increase with depth. Salinity is the stable component that keeps the stratification stable while the temperature term is unstable, and this leads to the diffusive layering mode of double diffusion. The effect of either modes of double diffusion is that an instability will lead to convection that will increase the vertical transport.

1.2.1 Salt Fingering

In order to understand salt fingering, visualize a thin vertical metal tube in the water column within a region of the ocean in which T and S both decrease with depth.

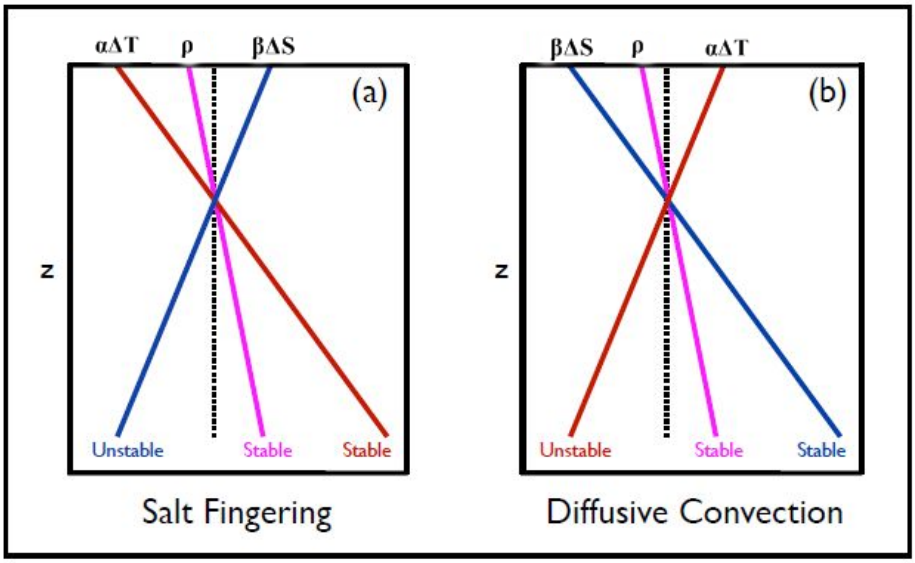

Figure 1.2: The 2 modes of Double Diffusion. In each subplot, the density (pink line) is stable relative to a vertical stability line (dashed), with density increasing downwards. However, in (a) the temperature contribution to density ($\alpha\Delta T$) from eq. 1.1 is also stable but the saline contribution ($\beta\Delta S$) is not. This leads to salt fingering. In (b) we show the opposite case, where $\beta\Delta S$ is stable but $\alpha\Delta T$ is not. This leads to diffusive convection (Scheifele, 2013).

The water parcels inside the tube are initially in thermal equilibrium with the surrounding water masses. Now if a water parcel is transported upwards slightly by some process it will be colder than the surrounding water masses and less saline. As heat conducts through the wall of the tube the parcel will come to a new thermal equilibrium so the parcel now warms but remains less salty. Therefore it is less dense than the surrounding water masses. Since it is less dense, it will continue to move upwards gaining heat but without becoming more salty, forming a finger (a similar process can result in downward fingers). Stommel (1956) first documented this phenomenon and stated that the seawater will keep rising until both temperature and salinity reach an equilibrium with the surroundings.

In the ocean there are no metal tubes but the different diffusivities can result in a "virtual" tube. This is because the diffusivity of heat in water is about a hundred

times greater than the molecular diffusivity of salt. Therefore the difference in the diffusive speed for the two constituents takes the place of the metal tube, allowing a water parcel to gain heat but not salt while it rises in the water column. However, salt diffusion will eventually set an upper limit at the length of the fingers.

Following the theory of Stommel, lab experiments proved that warm salty water above cold fresh water can form vertical fingers (Stern, 1960). Similar features were later seen in subtropical regions (Schmitt, 1994; Kelley et al., 2003).

1.2.2 Diffusive Layering Mode

In order to visualize the differences between the salt fingering mode and the diffusive layering mode, we first need to imagine that in this case temperature and salinity both increase with depth (the opposite of the salt fingering case). Interpreted in figure 1.2(b) we can discuss this system considering that heat diffuses faster than salt which will lead a water parcel displaced vertically downward to gain heat while the salt content will remain the same. The water parcel is now lighter and will start rising upwards in the water column until it loses the gained heat because the water column becomes colder as it rises. Therefore the water parcel begins to sink. An oscillation spontaneously arises.

The difference between the two modes is that in the salt fingering case the water parcel will keep rising without being more dense while in the diffusive layering mode it will rise and sink repeatedly because of the density changes.

Although at this point the detailed evolution of the instabilities are unclear, the eventual outcome of both modes is the signature structure of double diffusion: a staircase containing many steps (e.g., fig. 1.1). The existence of staircases is the primary way of recognizing the existence of the forcing of double diffusion in the ocean.

1.2.3 Physics of the Step

What is happening in this staircase? A diffusive instability staircase is composed of nearly homogeneous layers separated by thin interfaces. Heat diffuses faster through the interface than salt. As heat diffuses from the warm lower layer into the cold upper layer the fluid above the interface becomes lighter and the layer below

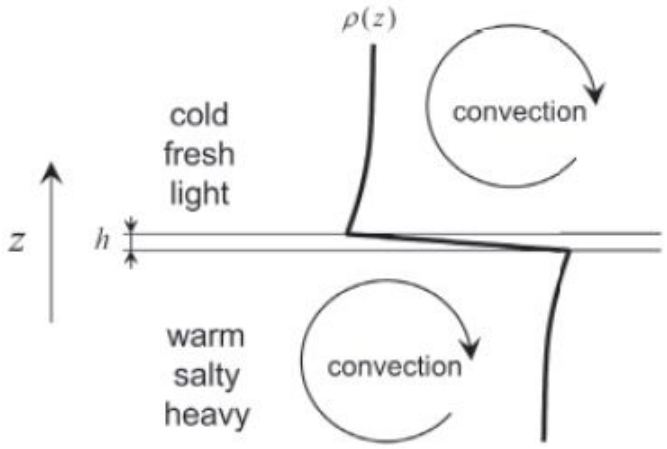

Figure 1.3: The double diffusive step

becomes more dense, forcing convection in both weakly stratified layers. The time scale for the generation of a convection overturn was investigated in Powell Lake B.C. by Zaloga (2015) who found that it was about 10 hours. After 10 hours convection will restore the sharp step and this process will start all over again for the next 10 hours.

These DD staircases involve simple diffusion across the steps. But seawater is a mixture of water (96.5%) and salt (3.5%) where salt itself is made up of many different constituents (the most abundant ones, which contribute the most to density, are chloride, calcium, sodium, sulfate, magnesium and potassium). Although a typical diffusivity for sea salt is 10^{-9} m^2/s, in fact the molecular diffusivities of the different ions vary by a factor of about 4 (fig. 1.4). Simple diffusion models do not take into account this complication. What is actually happening in this staircase is that at each step the different ions diffuse from the lower layer to the upper layer through the interface at different speeds. This makes the staircase a multicomponent system where multicomponent diffusion (MCD) processes are the most important forcing in this system.

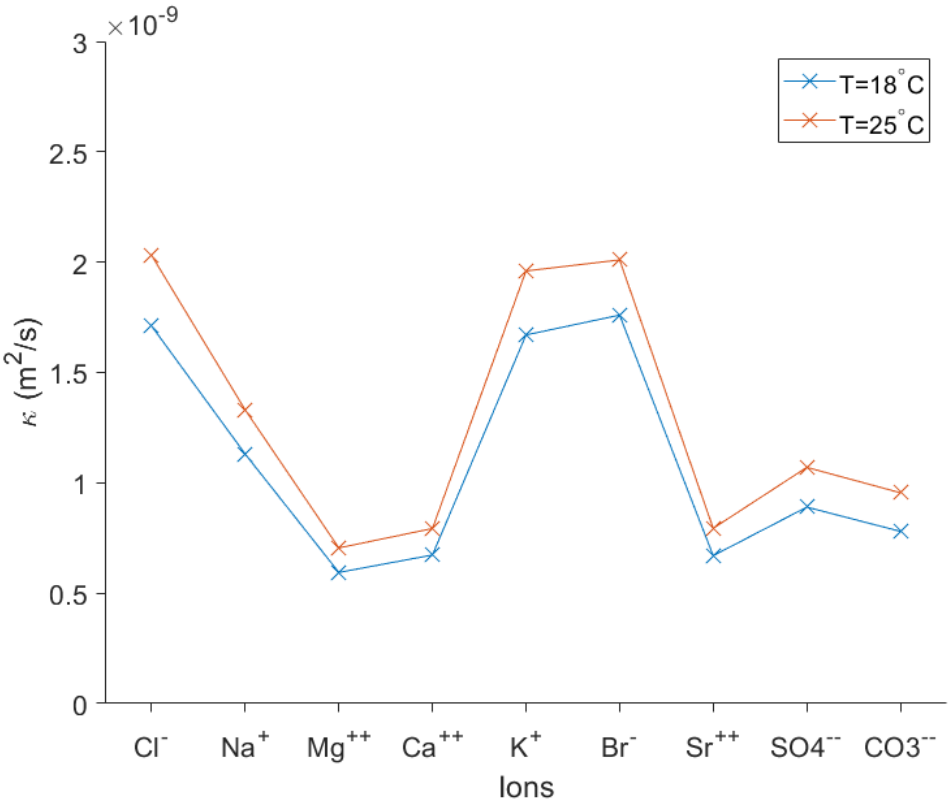

Figure 1.4: The diffusivities of different major ions in seawater at 18°C and 25°C. Values from Li and Gregory (1973)

.

We idealize this system by considering one step where ions will diffuse at different rates until convection will mix both layers and restore the step. Considering that the same physical processes apply to all steps we can simulate one step of this staircase in order to investigate the effect of MCD to the chemical composition above and below the step and the possibly different long-term effect on each ion.

1.3 Thesis Objective

Although many questions about Double Diffusion remain, the broad overview discussed above is generally accepted. However since diffusivities of ions differ

across the step, in this thesis we will attempt to answer the following question: Is it necessary to simulate a multicomponent system in order to model the diffusion of sea salt in DD staircases? And is MCD important is some areas in the ocean?

In a multicomponent system each ion may migrate at a different rate than the other ones and the different ions can interact with each other. Simulating one of the steps of the characteristic staircase (fig. 1.1) we investigate the effect of multicomponent diffusion and compare it to simple diffusion and single salt diffusion to show the differences that occur. We then discuss the results to determine whether these differences have significance for our understanding of ocean processes.

Our approach will be primarily numerical, but in order to test the conclusions of our model we will compare against observations in Powell Lake, Canada. Powell Lake is an excellent testing location considering that transport within the lake is primarily affected by DD processes (Scheifele et al., 2014). The lake contains ancient seawater (Mathews et al., 1970) but the current chemical composition is known to be slightly different than that of the ocean. The difference in the chemical composition may be due to the fractionation effect of multicomponent diffusion.

A simple multicomponent diffusion model was used by Sanderson et al. (1986) to study the general form of temperature and salinity profiles, as well as the chemical composition of Powell Lake. However, in their model they used the diffusion coefficients for each ion but did not account for any effects of ion charge for the ions resulting in possibly inaccurate conclusions.

Chapter 1 was an introduction to double diffusion, the theory and the physics behind the staircases and the complications that arise and lead us to use multicomponent diffusion in order to investigate this phenomenon that has attracted the attention of many scientists. In the following chapters we will discuss the theory behind our model simulation and the difference that occurs between treating salinity as single salt and as a mixture of ions.

Chapter 2

Methods

2.1 Multicomponent Diffusion Theory

As discussed in Section 1, we aim to simulate diffusion processes across a step. Not only do ions diffuse to reduce concentration gradients, but there are other more subtle effects that are involved related to thermal effects and ion/ion interactions. In this section we will determine which will be important in oceanic DD processes.

2.1.1 Fickian Diffusion

The simplest models of diffusion fluxes utilize Fick's first law,

$$J_i = -\kappa_i^* \nabla c_i \tag{2.1}$$

where κ_i^* is a diffusion coefficient, c_i is the molar concentration, and J_i is the diffusive flux for the i^{th} constituent in a multicomponent system. In eq. 2.1, the flux of the i^{th} component is only related to the concentration gradient of that component by a diffusion coefficient specific for that component. There are no interactions between any ions. The total flux J of salt in a multicomponent system with N species of dissolved solute would be:

$$J = \sum_{i=1}^{N} J_i \tag{2.2}$$

This may be sufficient for multicomponent systems that contain uncharged molecules. However, if the solution contains ions, then we have both positively and negatively charged and as they diffuse at different rates we may have areas that become predominantly positively (or negatively) charged, which as we will discuss later is not possible.

2.1.2 Chemical Potential

Although Fickian diffusion is based on concentration gradients, diffusion is more properly written in terms of chemical potential. The chemical potential of a chemical species in a non-ideal solution is a function of temperature, chemical concentration and an activity coefficient expressed as (Lasaga, 1979; Oelkers, 1996):

$$\mu_i = \mu_i^0 + RT \log \frac{\gamma_i c_i}{c_0} \tag{2.3}$$

where μ^0 denotes the chemical potential at a reference state, c_0 is a reference concentration for ideal behaviour, R is the gas constant and γ_i is the activity coefficient of the i^{th} chemical component. The activity is a factor used in chemistry to account for the differences in the behaviour of the ions between an ideal solution and a real solution where molecules can interact with each other. More details about activity are provided in appendix B, but molecular diffusion is more properly written as:

$$J_i = \kappa_i \nabla \mu_i \tag{2.4}$$

2.1.3 A Full Diffusion Equation

However, diffusive fluxes also arise from temperature gradients (thermophoresis or the Soret effect) and ions can also be affected by internal electric fields, which can be created as positive and negative ions diffuse at different rates (Felmy and Weare, 1991). Lasaga (1998) presented the total diffusive flux of a chemical component due to the chemical, electrical and thermal potentials based on the irreversible thermodynamics as:

$$J_i = -L_{ii}[\nabla \mu_i + F z_i \nabla \Phi] - L_{iq} \frac{\nabla T}{T} \tag{2.5}$$

L_{ii} is a phenomenological transport coefficient and L_{iq} is a transport coefficient of thermally induced chemical diffusion for the i^{th} chemical component. T is the temperature above absolute zero, F the Faraday constant, z_i the charge of ion i and Φ refers to the electrical potential in the solution, which can accelerate charged ions. Eq. 2.3 allows us to replace the chemical potential gradients with concentration gradients which are measurable, since:

$$\nabla \mu_i = \frac{\partial \mu_i}{\partial c_i} \nabla c_i + \frac{\partial \mu_i}{\partial T} \nabla T \tag{2.6}$$

Eq. 2.5 can then be expanded using eq. 2.6 as (Lasaga, 1998; Balluffi et al., 2005):

$$J_i = -L_{ii}[\frac{\partial \mu_i}{\partial c_i} \nabla c_i + F z_i \nabla \Phi] - \frac{L_{ii}}{T}[T \frac{\partial \mu_i}{\partial T} + \frac{L_{iq}}{L_{ii}}] \nabla T \tag{2.7}$$

where the term inside the second bracket in the coefficient for thermal diffusion is known as the heat of transport (Q):

$$Q_i = T \frac{\partial \mu_i}{\partial T} + \frac{L_{iq}}{L_{ii}} \tag{2.8}$$

The phenomenological coefficients of diffusion for each component L_{ii} can be approximated as (Lasaga, 1979; Oelkers, 1996):

$$L_{ii} = \frac{\kappa_i^0 c_i}{RT} \tag{2.9}$$

where κ_i^0 refers to the self-diffusion coefficient of the subscripted component in pure water calculated using the Nernst equation (Li and Gregory, 1973; Jost, 1960; Robinson, 1959):

$$\kappa_i^0 = -\frac{RT \lambda_i}{z_i F^2} \tag{2.10}$$

where λ_i is the equivalent conductivity at infinite dilution of ion i. Substituting the phenomenological coefficient using eq. 2.9 into eq. 2.7, following Lasaga (1979), the diffusion flux can be represented as:

$$J_i = -\frac{\kappa_i^0 c_i \partial \mu_i}{RT \partial c_i} \nabla c_i - \frac{\kappa_i^0 c_i F z_i}{RT} \nabla \Phi - \frac{\kappa_i^0 c_i Q_i}{RT^2} \nabla T \tag{2.11}$$

The first term on the right represents the effect of the concentration gradient, the second term the effect of electrical fields as positive and negative ions separate, and the third term is the thermophoresis effect.

2.1.4 Soret Effect

Thermophoresis is the phenomenon that is observed when molecules interact due to the effect of a temperature gradient. The consequence of this temperature gradient is that the particles will be forced to move from the warmer areas to the colder ones (Reinhardt and Kern, 2018). The term thermophoresis often apply to gaseous mixtures while when discussing liquid mixtures the more suitable term is the Soret effect. Charles Soret performed an experiment where he contained a salt solution in a tube with two ends of different temperatures and discovered that the solution did not remain uniform in composition. The salt's tendency to concentrate near the cold end of the tube suggested that a flux of salt was generated by a temperature gradient resulting in steady-state conditions, in a concentration gradient (Bouty, 1880).

In the third component of eq. 2.11, the Soret effect, the heat of transport Q_i is written by some authors as:

$$Q_i = RT^2 S^T (1 + \frac{\partial ln\gamma}{\partial lnc}) \tag{2.12}$$

where S^T is known as the Soret coefficient (Caldwell and Eide, 1985a). Neglecting the terms inside the brackets in eq. 2.12, i.e., assuming the activity coefficient as approximately constant, we can incorporate eq. 2.12 into the third component of eq. 2.11 and bring it to a form similar to the component used by Caldwell and Eide (1985b) to describe the Soret effect.

$$\frac{\kappa^0 cQ}{RT^2}\nabla T \approx \kappa^0 cS^T (1 + \frac{\partial ln\gamma}{\partial lnc})\nabla T \approx \kappa^0 cS^T \nabla T \tag{2.13}$$

In eq. 2.13 the left hand side represents the Soret effect component of eq. 2.11 and the right hand side represents the Soret effect component described by Caldwell and Eide (1985b).

The Soret effect in a multicomponent system as a part of the total diffusion of components was studied and researchers found that it is usually a small fraction of

the Fickian diffusion in seawater (Caldwell and Eide, 1985b), i.e., S^T is O(10^{-3}). Nevertheless, in some rare cases where temperature gradients are large the Soret effect is important (Caldwell and Eide, 1985b; Turner, 1969).

2.1.5 Electrical Potential Fluxes

As positive and negative ions are subject to diffusion forces of different strengths, there is a tendency for areas of predominantly positive (or negative) charges to arise when concentration gradients exist, which gives rise to electrical fields. However, Dickinson et al. (2011) finds that for any time longer than nanoseconds there is not enough Gibbs free energy in a chemical reaction to separate charge in an electrolytic medium. Instead the electric fields that arise are strong enough to prevent charge separation. Based on that it is valid to assume a quasi-steady electroneutrality in our system. Thus, we must have an additional zero current constraint:

$$\sum_{i=1}^{N} z_i J_i = 0 \tag{2.14}$$

Incorporating this condition in eq. 2.11 where we only use the diffusive and electrical potential terms we can derive the gradient of electrical potential. This zero current flows only if:

$$\nabla\Phi = -\frac{RT}{F}\left[\frac{\sum_{i=1}^{N} z_i \kappa_i^0 c_i \frac{1}{RT}\frac{\partial \mu_i}{\partial c_i}\nabla c_i}{\sum_{i=1}^{N} z_i^2 \kappa_i^0 c_i}\right] \tag{2.15}$$

In the case of a binary solution, e.g., $NaCl$, both Na^+ and Cl^- ions are forced to diffuse at the same rate (Appendix C). This implies that in a multicomponent system, an electrical potential is formed by the diffusion of ions across an interface. This is also called a "liquid junction potential"(LJP).

2.2 Relative Importance of the Three Terms

The total diffusive flux of each ion, as described in eq. 2.11, depends on three different components, the concentration gradient effect, the electrical fields effect and

the Soret effect. In order to estimate the relative importance of the three components in seawater situations we now try to estimate the approximate magnitude of each term for Na^+ using the scales seen in the deep seawater-filled part of Powell Lake (fig. 1.1).

For scaling purposes we take the activity coefficient of sodium to be approximately constant since its variation is small. By making this assumption,

$$\frac{\partial \mu_i}{\partial c_i} \approx \frac{RT}{c_i} \tag{2.16}$$

and the first component, the concentration gradient effect, of eq. 2.11 becomes:

$$-\frac{\kappa_i^0 c_i \partial \mu_i}{RT \partial c_i} \nabla c_i \approx -\kappa_i^0 \nabla c_i \tag{2.17}$$

Therefore we can use the values from table 2.1 in order to scale the first component. The ∇c component is calculated for the concentration of sodium above and below the 10 cm thick interface where Δc is basically the concentration difference for the salinity difference (ΔS):

$$\Delta c = \frac{\Delta S}{S} c \tag{2.18}$$

At a distance of $\Delta z = 10^{-1}$m with the concentration difference (Δc) being 10^{-3} mol L^{-1} we can evaluate ∇c to be in the order of 10^{-2} mol L^{-1} m^{-1} and we find that the purely diffusive flux is in the order of 10^{-11} mol m^{-2} h^{-1}.

For the second component, the electrical fields effect, all the parameters are listed in table 2.1 and we use them in order to make our scaling. We do not know $\Delta\Phi$, but Easley and Byrne (2012) found that LJP were on the order of 10^{-4}V, which we take as a typical value here. Therefore $\nabla\Phi$ is on the order of 10^{-3} V m^{-1} and the electrical potential driven flux is in the order of 10^{-12} mol m^{-2} h^{-1}.

The third component, the Soret effect, can be written as:

$$\frac{\kappa^0 c Q}{RT^2} \nabla T = \kappa^0 c S^T \nabla T \tag{2.19}$$

where the Soret coefficient is in the order of $10^{-3}K$ (Caldwell and Eide, 1985a). The last term (∇T) is on the order of $10^{-2}K$ m^{-1} with the temperature difference

(ΔT) being in the order of $10^{-3}K$ for a distance (Δz) of 10^{-1}m. Therefore transport due to the Soret effect is in the order of 10^{-17} mol m^{-2} h^{-1}.

Thus, we find that the diffusive flux is in the order of 10^{-11} mol m^{-2} h^{-1} while the electrical potential flux is in the order of 10^{-12} mol m^{-2} h^{-1} and the Soret effect is in the order of 10^{-17} mol m^{-2} h^{-1}. The Soret effect, which has been studied in seawater (Caldwell and Eide, 1985a), is apparently not very important in our case and can be neglected. On the other hand, the second component, the electrical potential effect (which is also essential to maintain charge balance) may be important.

Although the electrical potential effect has not been studied in seawater, it has been investigated in other systems. Lasaga (1998) investigates the multicomponent diffusion and exchange in silicates. This work accounts for the chemical and electrical potential driven fluxes and discusses the cation exchange in complex silicate systems.

Giambalvo et al. (2002) study how the fluid–sediment reactions affect the hydrothermal fluxes of major elements in groundwater and they include the electrical potential driven fluxes in their total diffusive fluxes accounting for electrochemical migration. This work investigates the changes in the rates of the hydrothermal fluxes due to the effect of fluid-sediment processes but does not separate the electrochemical fluxes in their results in order to see the effect and fraction of electrical potential driven fluxes to the total flux.

Rasouli et al. (2015) described three different benchmarks for experiments of diffusion and electromigration in order to describe the effect of these two fluxes in *NaCl* environments. This work primarly tries to estimate the accuracy of three different reactive transport models but also shows the effect of the electrical potential driven fluxes which tends to speed up the positively charged ions while it slows down the negatively charged ions.

The work of Muniruzzaman et al. (2014) investigates the effects of Coulombic interactions during transport of electrolytes in heterogeneous porous media. Here, the authors estimate the electrical potential driven fluxes and also notice that it tends to speed up the positively charged ions and slow down the negatively charged ones. This work states that it is important to improve the understanding of electrochemical migration of charged species in geologic formations.

Table 2.1: The values for the parameters used in order to estimate the relative importance of the three components forming the total flux for one of the ions (sodium)

Parameter	Value	Units
Temperature T	282.15	K
Gas Constant R	8.3147	J K^{-1} mol^{-1}
Faraday Constant F	10^5	C mol^{-1}
Diffusion Coefficient D^0	10^{-9}	m^2 s^{-1}
Charge Number z	+1	-
Activity Coefficient γ	0.7193	-
Concentration c	10^{-1}	mol l^{-1}
S^T (Caldwell and Eide, 1985a)	10^{-3}	K^{-1}
∇c	10^{-2}	mol l^{-1} m^{-1}
ΔT (Scheifele, 2013)	10^{-3}	K
$\Delta\Phi$ (Easley and Byrne, 2012)	10^{-4}	V
Δz (Scheifele, 2013)	10^{-1}	m

Shiba et al. (2005) developed a mathematical model for electrokinetic remediation in soil and groundwater. With this model the effect of electromigration on the removal of heavy metals was investigated and found to be effective for the redistribution of heavy metals through effluent.

2.3 Numerical Implementation

Researchers who study the flow, transport and reaction processes in porous media are increasingly using reactive transport models. These models aim to simulate processes by interpreting real data in the fields of geology, engineering and environmental sciences (Boudreau, 1997; Kang et al., 2006; Wang and Van Cappellen, 1996; Steefel et al., 2003). An extension is Fickian diffusion, where the diffusion coefficients can be adjusted as different parameters (Cussler, 2009). Although the use of these reactive transport models has been initiated a few decades ago, only in recent years has electromigration begun to be included in the models and the chemical potential gradient considered to be the driving force for diffusion (Lasaga, 1998; Giambalvo et al., 2002; Johannesson et al., 2007; Muniruzzaman et al., 2014; Parkhurst et al., 1999; Paz-García et al., 2011; Shiba et al., 2005).

A multicomponent diffusion model that incorporates the physics mentioned above is MIN3P (Mayer et al., 2002; Rasouli et al., 2015). MIN3P is a multicomponent reactive transport model for variably-saturated porous media that is capable of simulating from one to three dimensions with multicomponent diffusion being one of its possible extensions in saline solutions. The model is characterized by a high degree of flexibility in order to make the model applicable to various hydrogeological and geochemical problems. In our usage of MIN3P we restrict ourselves to a 1-D problem with no advection. Details on the model's setup are provided in Appendix A.

Chapter 3

Multicomponent Diffusion in Powell Lake

3.1 Study Area

The intention of this work is to investigate multicomponent diffusion transport in order to better understand its effect on the chemical composition of seawater. To properly study this process observationally we require a relatively stable oceanic region where the main force provoking changes in the chemistry of the environment will be diffusive transport. Osborn (1973) hypothesized that the double diffusive instability may be active in the deepest parts of Powell Lake B.C., which despite its name contains seawater, and this was confirmed by Scheifele et al. (2014). The major ion composition of the seawater in the lake was first studied by Sanderson et al. (1986), and since it is slightly different than that of present-day seawater it suggests that MCD may be able to affect seawater composition in regions where diffusion processes are important.

3.1.1 Powell Lake

Located 150 km north of Vancouver (fig. 3.1), Powell Lake is a glacially formed ex-fjord about 40 km long with a maximum depth of 350 m. The lake was originally a marine fjord but with the melting of the Cordilleran Ice Sheet the lake was formed

due to the rise of a sill at the mouth of the fjord (Scheifele, 2013). Historical data suggest that seawater was trapped in the lake between 12,500 and 10,500 years ago (Mathews et al., 1970) during a period of relatively rapid coastal uplift (Clague and James, 2002). The bottom of the lake is anoxic below 125 m depth (Perry and Pedersen, 1993) and the surface is 50 m above sea level.

Mathews (1962) carried out a bathymetric study of the lake and determined that it contains six basins. Two of those, the east and south basins, are permanently stratified and contain warm relic seawater. Williams et al. (1961) discovered the presence of seawater in the lake and high concentrations of sulphide in the deep anoxic regions of the lake.

Freshwater input to Powell Lake by river runoff mostly occurs at the northern head of the lake. However shallow sills separate the lake's basins, trapping any turbidity currents and isolating them to the northern areas, thus protecting the southern regions containing relic water from mixing. The southern lake is separated from the sea by a rocky sill where a hydroelectric dam which was built in the early 20th century, which stabilized the level of the lake at approximately about 7 m higher than its natural level.

Sanderson et al. (1986) assumed that molecular diffusion and eddy diffusion were the main vertical transport mechanisms in the lake for heat and salt and successfully attempted to model the evolution of the lake and reproduce current temperature and salinity profiles in the south basin of the lake. Diffusion transports heat and salt from the bottom of the lake to upper layers. Temperature decreases with depth until approximately 125 m where the lake becomes anoxic and then starts to increase with depth reaching a maximum of 9°C at the bottom. The reason behind the increase of temperature with depth is a geothermal heat flux into the bottom of the lake. Hyndman (1976) measured the flux to be approximately 27 mW/m^2 in the sediment.

Salinity is almost zero from the surface down to a depth of 125 m, and then starts increasing with depth until a maximum value of 17g/kg is reached at the bottom. Between 300 and 350 m double diffusive staircases were observed in high-vertical-resolution hydrographic profiles suggesting that double diffusion is the main transport mechanism in that deep region of the lake (Scheifele, 2013).

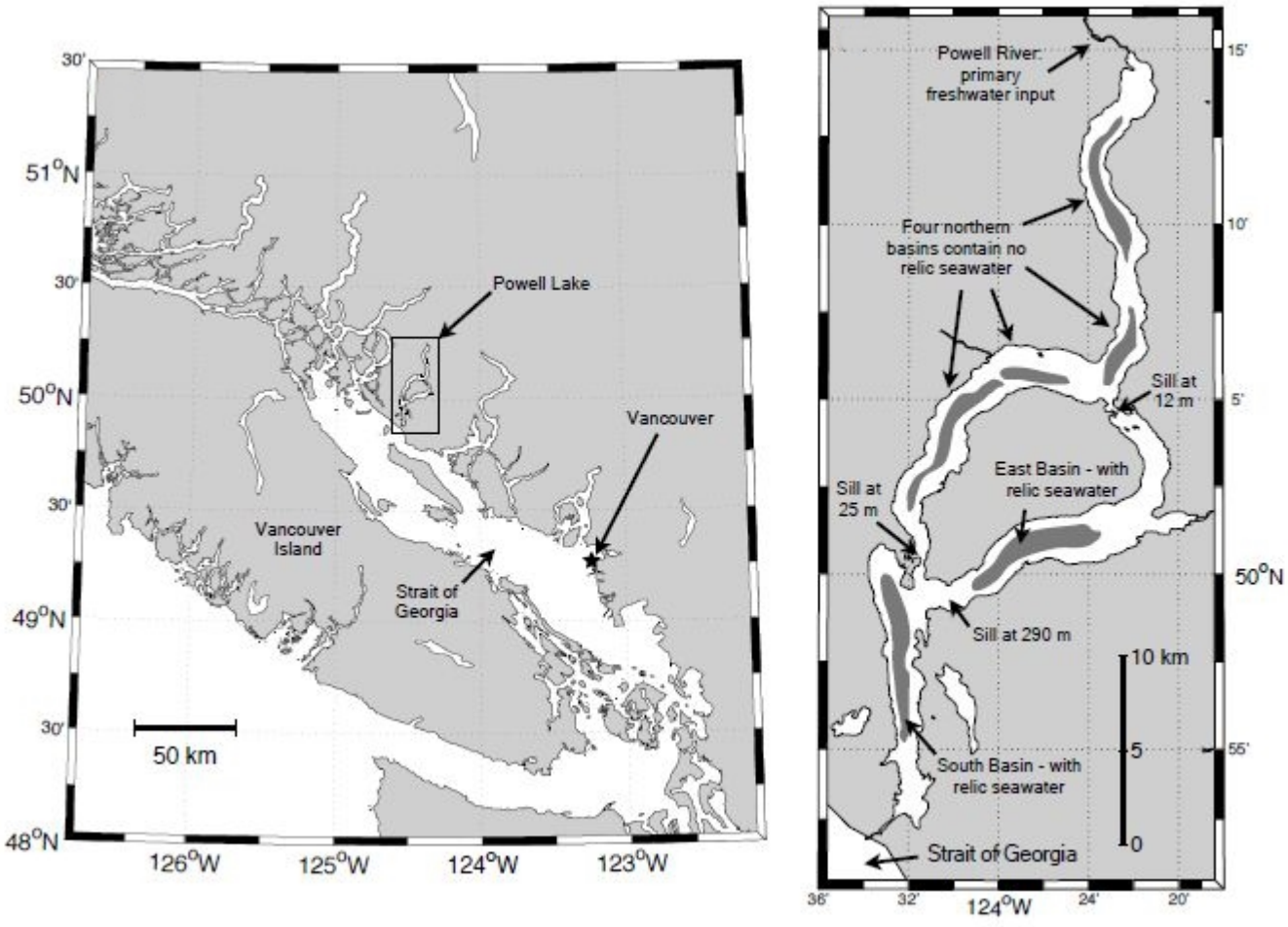

Figure 3.1: Powell Lake in British Columbia (Scheifele, 2013)

3.2 Our Approach

We will numerically simulate a single Multi-diffusive step using the MIN3P code in order to understand the consequences of MCD without the complications of modelling an entire diffusive/turbulent staircase. Investigating a single step of the staircase, will provide us the necessary information regarding the effect of the different diffusion rates of the ions to the chemical composition of seawater. As a first step, we will run a simulation in order to investigate the effect of having multiple

ions diffusing through the interface for 10 hours which, as we mentioned in sec. 1.2.3 is the timescale between turbulent convection events that sharpen the step. Then, considering the physics of the step, we want to run a different simulation in order to calculate the loss of ions from the lower layers of the lake to the surface water masses with time.

The salinity of the water around the step that we simulate is approximately 16.66g/kg with a step of 0.01g/kg and the temperature is 9°C (fig. 1.1). We set the model with the initial concentrations above and below the theoretical DD step according to fig. 1.1 simulating the real differences in salinity between the DD steps in Powell Lake.

To calculate the concentrations of individual ions from salinity we use the chemical composition of seawater as reference (Millero et al., 2008) and measured concentrations from Powell Lake water samples from 2010 that were estimated by laboratory work. We modified this by taking only the 10 most important ions and charge balanced the composition by slightly changing Cl^-. These include (table 3.1) Cl^- and Na^+ which are the two most abundant ions in seawater. Together, they make up almost 90% of sea salt. We also select Mg^{+2}, Ca^{+2}, SO_4^{-2}, K^+, Br^- and Sr^{+2} and all together, these 10 ions, make up more than 99% of sea salt. We also include the CO_3^{-2} and HCO_3^- which we consider as two separate decoupled ions in our model, and we represent them as Dissolved Inorganic Carbon in our results (DIC).

However, Powell Lake deep water is anoxic and chemical processes are known to have reduced sulfates to sulfides which then precipitate (Perry and Pedersen, 1993), and may have caused changes in the carbonate system as well. However, concentrations of these components are small relative to the concentration of the most abundant ions in seawater. We do not believe that this inclusion in our model will cause changes to our conclusions about Powell Lake, and keeping the model seawater closer to the open-ocean composition will let us discuss implications for the global ocean with more detail.

Although MIN3P can numerically solve the required equations, its use requires diffusion coefficients for all the ions for a temperature of 9°C. In order to estimate these we use their relationship to ionic conductivity (eq. 2.10), obtaining the required conductivity from the LIMCOND numerical model (Pawlowicz, 2008). The

method is similar to that used by Li and Gregory (1973) where the diffusivities of ions are calculated based on the Nernst equation. Unfortunately, Li and Gregory (1973) do not include the diffusivities of the ions for T=9°C but only for T=18°C and T=25°C. Therefore we also calculate the diffusivities for the ions for T=18°C and T=25°C. Comparing our results with the estimation of the diffusivities from Li and Gregory (1973) we see that the relative difference in the resulting diffusivities is on the order of 10^{-4} (fig. 3.2). The calculated values at 9°C are lower than those at 25°C by 35-40%.

The simulations are first performed using a full MCD process. However, in order to estimate the effects of the electric fields we repeat our calculations with several simplified models of diffusion. First, we use "single diffusion" in which different ions diffuse at their intrinsic rates with no ion/ion interactions. Second, we use a "single salt" model where all ions have the same diffusivity.

We set the different concentrations for the selected ions in two regions of the box model and define a 1-D setup for the modelover a distance of 2 m in total (1 m for each one of the two regions, one above and one below the step). The number of grid points is set to 500 for z: 0-0.8 m, 500 for z: 1.2-2 m and 1000 grid points between 0.8-1.2 m in order to focus more on the important region which is the interface of the two layers. The boundary conditions of the model at the top and bottom of the region are set to be the initial values for each ion.

3.3 Results

3.3.1 Effective Diffusivities

A way of understanding the effect of ion/ion interactions is to start again with eq. 2.1, which suggests that:

$$\kappa_i^* = \frac{J_i^{Fickian}}{\nabla c_i} \tag{3.1}$$

Using MIN3P, we now have a more accurate representation of the fluxes J_i, so we can define an effective diffusivity in seawater, κ_{eff} as:

$$\kappa_{eff} = \frac{J_i}{\nabla c_i} \tag{3.2}$$

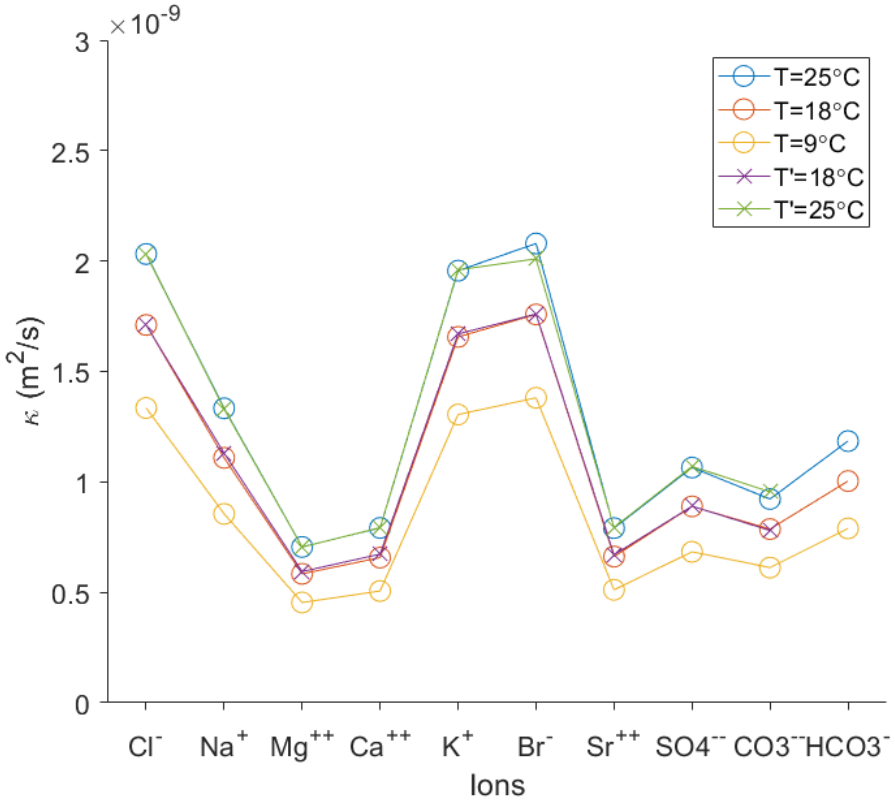

Figure 3.2: Comparison of the calculated diffusivities for T=9,18 and 25° C with the Li and Gregory (1973) estimated diffusivities for T'=18 and 25° C

using the calculated J_i and ∇c_i which we discuss in more detail later. If we now compare κ_i^* and κ_{eff} (fig. 3.3), we see that the negative ions have a decreased diffusivity, and the positive ions an increased diffusivity. This positive contribution of the electrical potential to the cations and the negative contribution to the anions has also been seen in other studies (Rasouli et al., 2015; Rolle et al., 2013). Also, for Na^+ and Cl^-, the most significant components, effective diffusivities are almost equal to 1×10^{-9} m^2/sec and for many of the ions, their diffusivities are modified to approach this value. However, sulfate ends up diffusing even less, and potassium even more.

Table 3.1: The concentration used for each ion in mol/l for the different salinities

Concentrations for the different salinities (mol/l)				
Ion	S=0.00001g/kg	S=16.6g/kg	S=16.7g/kg	S=35g/kg
Cl^-	1.56e-07	0.2591	0.2606	0.5462
Na^+	1.34e-07	0.2225	0.2239	0.4692
Mg^{2+}	1.5e-08	0.0250	0.0252	0.0528
Ca^{2+}	2.93e-09	0.00487	0.0049	0.0103
K^+	2.91e-09	0.00484	0.0048	0.0102
Br^-	2.4e-10	3.99e-4	4.01e-4	8.42e-4
Sr^{2+}	2.5e-11	4.29e-5	4.32e-5	9.06e-5
SO_4^{2-}	8e-09	0.0134	0.0135	0.0282
CO_3^{2-}	4.9e-10	8.14e-4	8.19e-4	0.0017
HCO_3^-	6.8e-11	1.13e-4	1.14e-4	2.39e-4

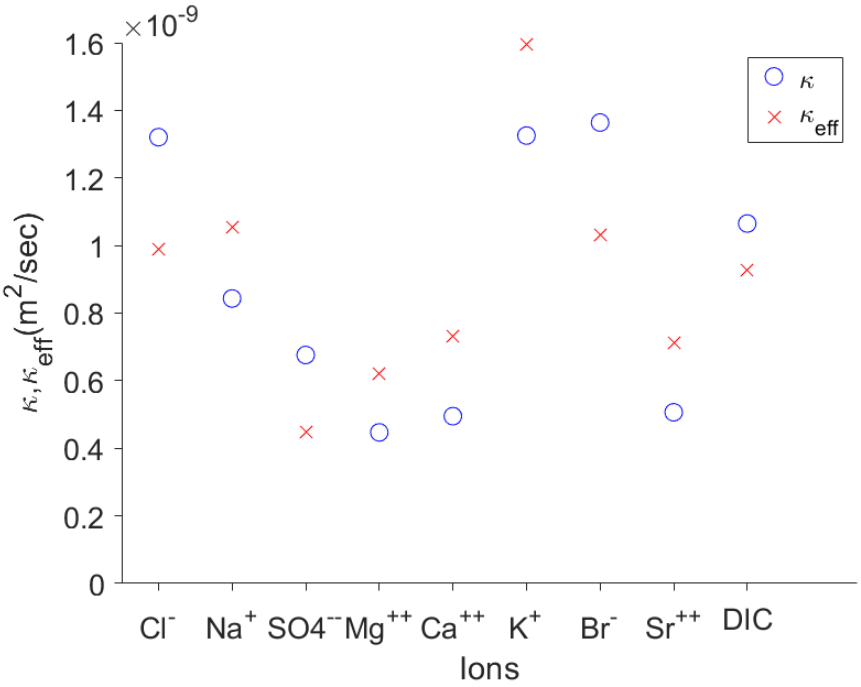

Figure 3.3: Diffusion coefficients for all ions before and after the effect of the electrical potential

3.3.2 Single Step - 10 Hours

The concentration gradient of the 10 ions, after diffusing from the lower layer of the step to the upper layer for 10 hours, reflects the fact that the different ions diffuse at different rates (fig. 3.4). Potassium diffuses faster than the rest of the ions and sulphate has the slowest diffusion. Most ions show a profile that looks like the error function (erf):

$$erf(x) = \frac{2}{\sqrt{\pi}} \int_0^x e^{-t^2} dt \tag{3.3}$$

which is typical for diffusive processes with a constant diffusivity initialized with a step. Sulfate, on the other hand, shows slightly elevated levels at z=0.985 (and a corresponding minimum at z=1.015).

The fluxes that apply to each ion's concentration gradient are the summation of the diffusive and electrical potential driven fluxes (fig. 3.5):

$$J_i = -\frac{\kappa_i^0 c_i \partial \mu_i}{RT \partial c_i} \nabla c_i - \frac{\kappa_i^0 c_i F z_i}{RT} \nabla \Phi \tag{3.4}$$

The two terms of this flux and the total flux for each ion after 10 hours are shown as a function of depth in fig. 3.5. The effect of the electrical potential is to slow down the negatively charged ions and speed up the positively charged ions. The electrical potential driven flux varies between 15-25% of the total flux. Each of the two flux terms have an approximate gaussian shape, but the width is different for the two terms. This leads to the max/min levels for sulfate where the width differences are large and terms have opposing sign.

3.3.3 Simple Diffusion

In order to run the model for the case of simple diffusion we need to exclude the effect of the electrical potential from our simulation. To do so, we have to run the model separatively for the 10 ions diffusing from the lower region to the top with the only thing affecting the diffusion rate being the selected diffusivity. The diffusivity (κ) of each ion for the simple diffusion case will be different than the effective diffusivity (κ_{eff}) for the multicomponent diffusion case by 20-40% since there is no electrical fields effect (fig. 3.6).

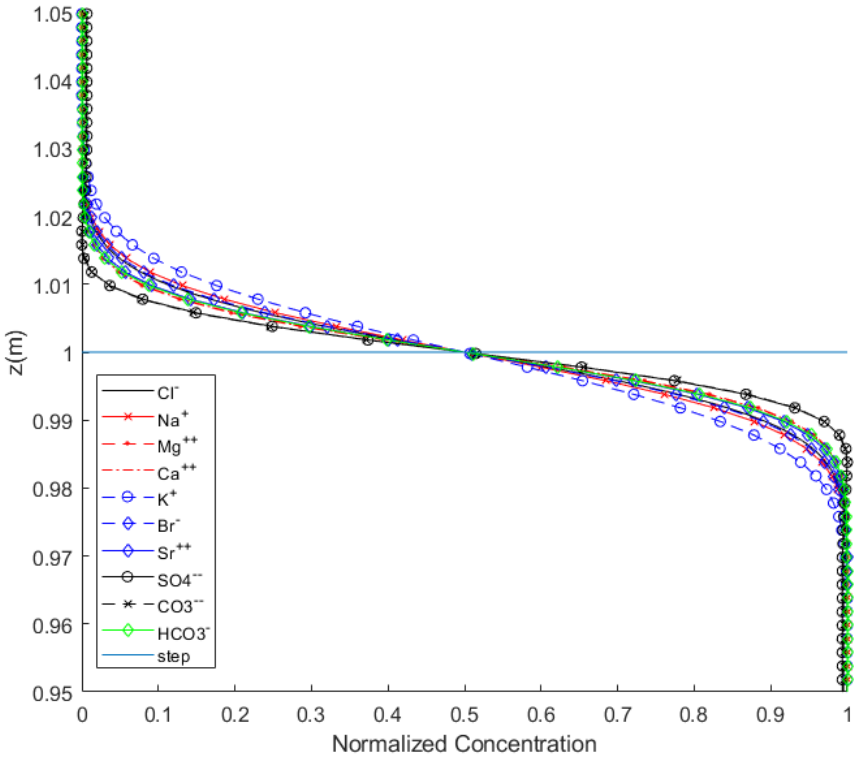

Figure 3.4: Molecular diffusion across the step for each ion. A result of the multicomponent diffusion model for an output time of 10h. The concentrations are normalized in order to bring all values in a range from 0 to 1.

In the simple diffusion case, all ions are diffusing following an erf-shaped curvature with a slight change between their fluxes which depends only on the first term of eq. 3.4. In this case sulfate is also following a similar curvature since there are no electrical fields affecting it. Comparing SD with MCD we see that the major difference in the two approaches is that there are no electric fields affecting a simple diffusive system, and their diffusivities are not increased or decreased. Therefore inaccuracies arise as we will discuss later.

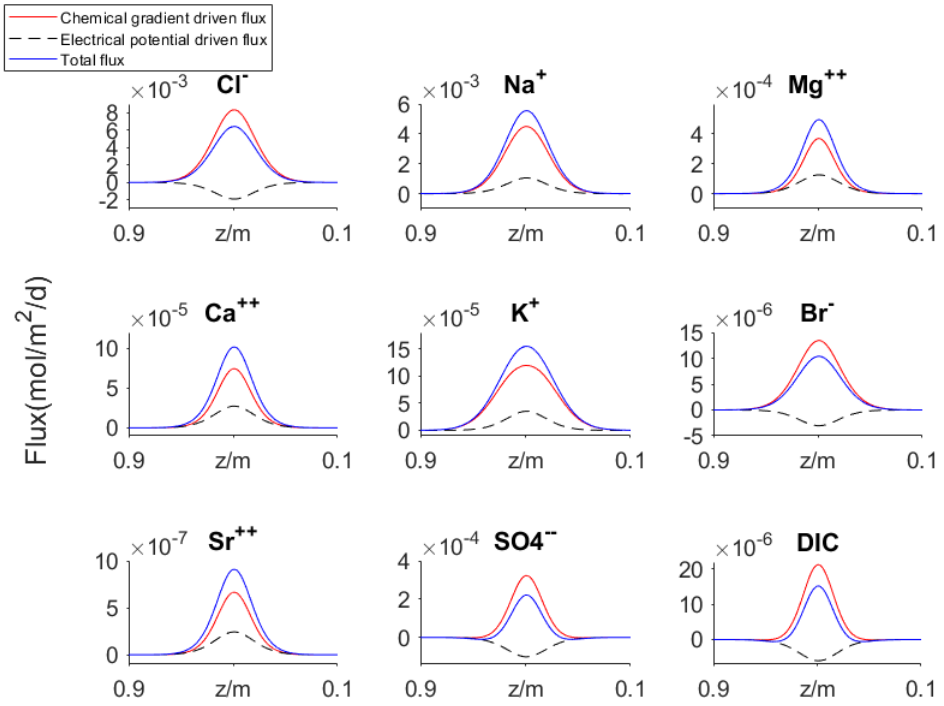

Figure 3.5: Diffusive and Electrical Potential driven fluxes and Total flux for each ion at the interface above and below the step. DIC is the summation of the carbonate and bicarbonate fluxes in order to show the dissolved inorganic carbon flux.

3.3.4 Single Salt Diffusion

For single salt diffusion we run the model with an identical diffusion coefficient for all ions. For the diffusivity of salt we choose the diffusivity of *NaCl* simply because sodium and chloride are the two most abundant ions in the ocean. We use the diffusivities of sodium and chloride to calulate the diffusivity of *NaCl* for 9°C using the formula (Li and Gregory, 1973; Jost, 1960):

$$\kappa_{NaCl} = \frac{(|z_{Na}| + |z_{Cl}|) * \kappa_{Na}\kappa_{Cl}}{|z_{Na}| * \kappa_{Na} + |z_{Cl}| * \kappa_{Cl}} \tag{3.5}$$

The derivation of this equation following the math in the previous sections can be seen in appendix 3 and it reaches the same result as following the Nernst-Haskell

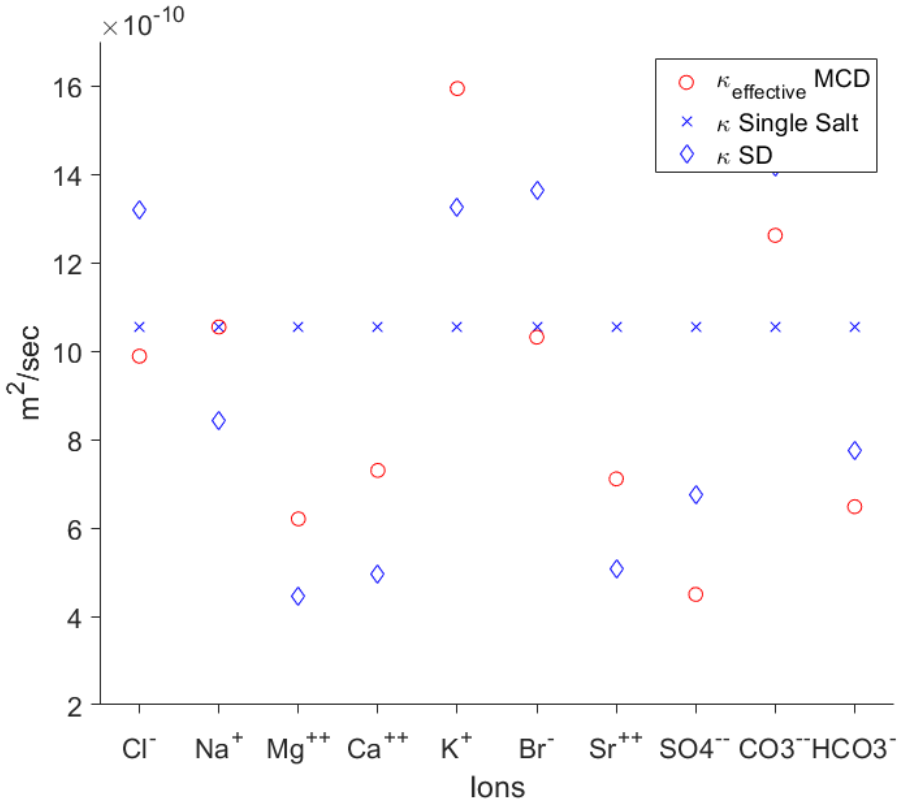

Figure 3.6: The diffusivities for Multicomponent Diffusion (MCD), Simple Diffusion (SD) and single salt (*NaCl*).

derivation (Poling et al., 2001).

Therefore, all ions diffuse at the exact same rate since they share the same diffusivity (fig. 3.6) and this leads them to follow the same erf-shaped curvature and there is no difference for sulfate or any other ion. The fluxes are now only depending on the first term of eq. 3.4 and there is not any change between positively or negatively charged ions. Comparing the single salt case with MCD we see that the major difference in the two approaches is that the electric fields which tend to speed up or slow down the diffusivity of the ions are not affecting the single salt system.

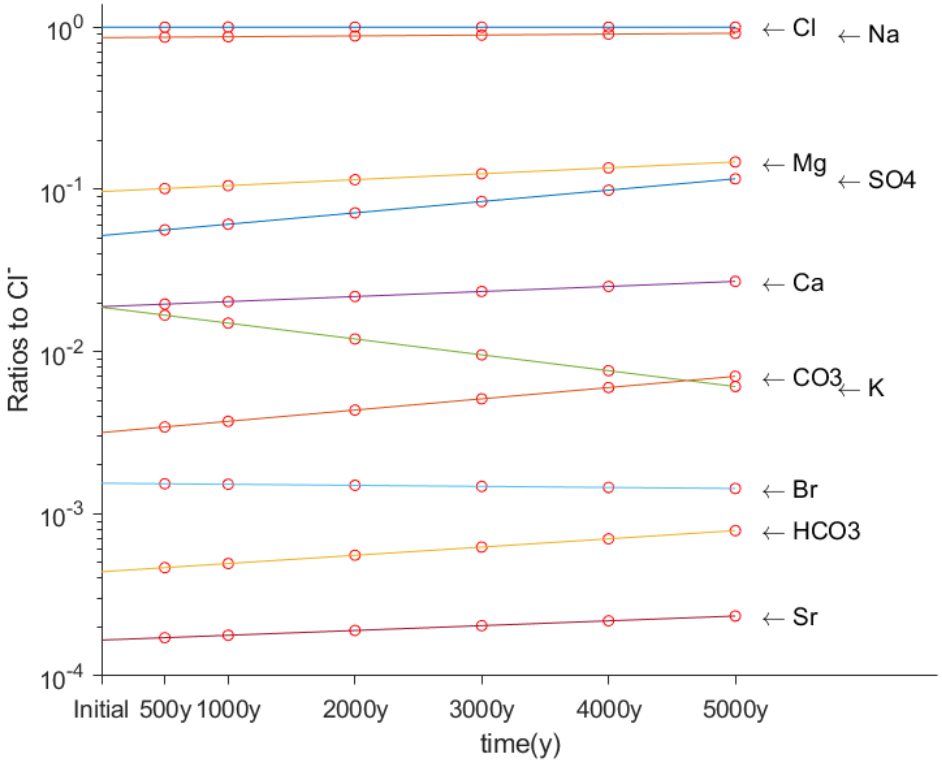

Figure 3.7: The changes in the concentration of ions, expressed as a ratio to the concentration of chloride, over time due to the effect of multicomponent diffusion.

3.3.5 Long-Term Effects

Since under the MCD processes different constituents diffuse at different rates, there is a weak fractionation that occurs. The lake is 350 m deep and the bottom water is salty while the surface waters are fresh and this has lasted thousands of years. However, the salinity of the lake bottom is much less than that of seawater in the Strait of Georgia. Thus, we infer that salt has been lost through diffusion processes and we want to see the changes in the chemical composition with time. We keep all the model's settings the same and we calculate the chemical composition of the lake starting at S=35g/kg after long periods of time if the transport

in the lake is being controlled by simple diffusion. Then we calculate the ratios to the initial values and we compare to the MCD's result. For the long-term simulation we set the length of the z-direction to be 0-300 m for the top part with a salinity of 0.00001g/kg and 300-320 m for the lower part with a salinity of 35g/kg. We set those numbers for the z-direction looking at the CTD casts of Scheifele (2013) from Powell Lake where we can identify where the double-diffusive staircases appear. Running the model with this setup will give us the information for the changes in concentration above and below the step for 10h (the approximate time scale of turbulent renewal). We use the average of the concentration below the step to see the amount that is lost for each ion and calculate the percentage lost for 10h.

Through a single step, over 10 hours, a fraction x_i where:

$$\int_{z=300}^{320} c_i(final) - c_i(initial)dz = \int_{z=300}^{320} (\frac{c_i(final)}{c_i(initial)} - 1)dz \times c_i(initial) = x_i c_i(initial) \tag{3.6}$$

has moved upwards before the diffused step is reestablished by turbulence. If we start with an initial concentration of c_i at the bottom of the lake, this implies that the concentration at some longer time T later will be:

$$c_i(T) \approx (1 - x_i)^n c_i(initial) \tag{3.7}$$

where $c_i(T)$ is the concentration of ion i at some time T, x_i is the percentage lost of ion i after 10 hours and $n = T/10$ hours. In turn, the relative composition of seawater, given by the ratio to the concentration of chloride will also change with time, and over time the initial fractionation will amplify (fig. 3.7):

$$\frac{c_i(T)}{c_{cl}(T)} \approx \left[\frac{1 - x_i}{1 - x_{cl}}\right]^n \frac{c_i(initial)}{c_{cl}(initial)} \tag{3.8}$$

where $c_{cl}(T)$ is the concentration of Cl after some time T, x_{cl} is the percentage lost of Cl^- after 10 hours and $c_{cl}(initial)$ is the initial concentration of Cl. Note that x_i is not sensitive to the value of $c_i(initial)$. x_i changes by less than 1% at initial salinities of 0.00001g/kg to 16g/kg. We start with a salinity of 35g/kg for seawater and we run our 3 different approaches of diffusion with time and compare our results to the lake's current composition.

Thus, we estimated the relative difference between ratios to initial value for 7 ions from our model's three approaches and the ratios to initial value from Powell Lake's measurements, in order to see how they vary with time (fig. 3.8). We exclude the sulphate, carbonate and bicarbonate ions from this analysis because they are affected by other processes that we do not include in our simulations. We see that the model's ratios will match the observed Powell Lake ratios at different timescales for each individual ion. For the Single Salt approach (fig. 3.8a), we see that the times at which ratios match (a relative difference of zero) cover a range of between 1760-6755 years with the majority of the ions matching somewhere between 4000-6000 years. For the Simple Diffusion case (fig. 3.8b), we see that only a few ions (K^+, Cl^- and Br^-) show a minimum difference between 2200-3200 years. Also, matching for Na^+, Mg^{2+}, Ca^{2+} and Sr^{2+} will not occur for at least 8000 years. For the Multicomponent Diffusion approach (fig. 3.8c), the range of matching ratios is slightly smaller, between 2215-6450 years with most of the ions again showing a timescale of best accuracy between 4000-6000 years.

To summarize, we see that none of the three approaches matches perfectly Powell Lake ratios. In the SD approach it will take some ions many more thousands of years to match Powell Lake ratios than others while in the Single Salt and MCD approaches it seems that the range is comparably smaller with the MCD approach having the closest matching values.

Then, we also compare two other statistical methods, the Mean Absolute Error (MAE) and the Root Mean Square Error (RMSE), in order to make an estimation over the average difference between the ratios from our three approaches and the Powell Lake's ratios (fig. 3.9).

For the MAE:

$$MAE = \frac{\sum_{i=1}^{N} \mid Ratios_{MCD} - Ratios_{Powell} \mid}{n} \tag{3.9}$$

For the RMSE:

$$RMSE = \sqrt{\frac{\sum_{i=1}^{N} (Ratios_{MCD} - Ratios_{Powell})^2}{n}} \tag{3.10}$$

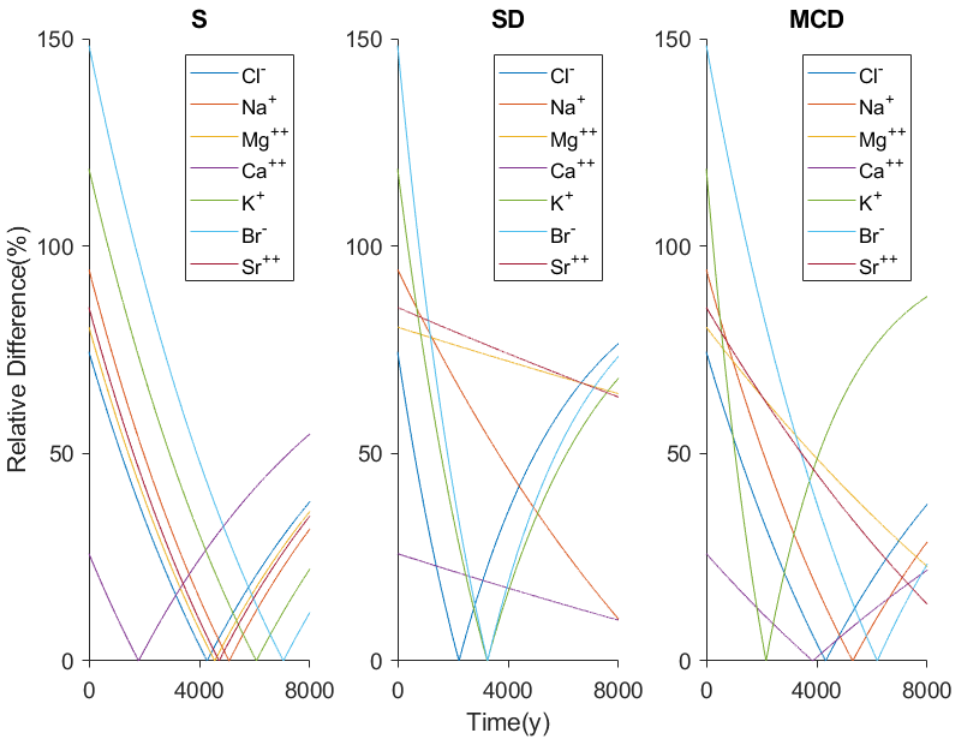

Figure 3.8: The relative difference of ratios to initial value of the ions between Powell Lake's measurements and our three approaches.

We see that the average timescale for the ratios of the S and MCD approaches, which provides a better match with Powell Lake's measurements, according to the MAE method is approximately between 4000-6000 years. This is also the case for the MCD approach in the RMSE method where the S case lacks the ability to give us some precise timescale. Therefore, from fig. 3.8 and fig. 3.9 it seems reasonable that we choose our timescale for the estimation of the long-term effects and our comparison of the three different approaches for diffusion to be 5000 years. Although 5000 years is less than 10.000 years which observations suggest has occured, note that the 10 hour turbulent time scale may be inaccurate.

In fig. 3.10 we show the effect of Multicomponent Diffusion (MCD), Simple Diffusion (SD) and Single Salt diffusion (S) on the chemical composition of the lake after 5000 years, and we compare the ratios of the concentration for each ion

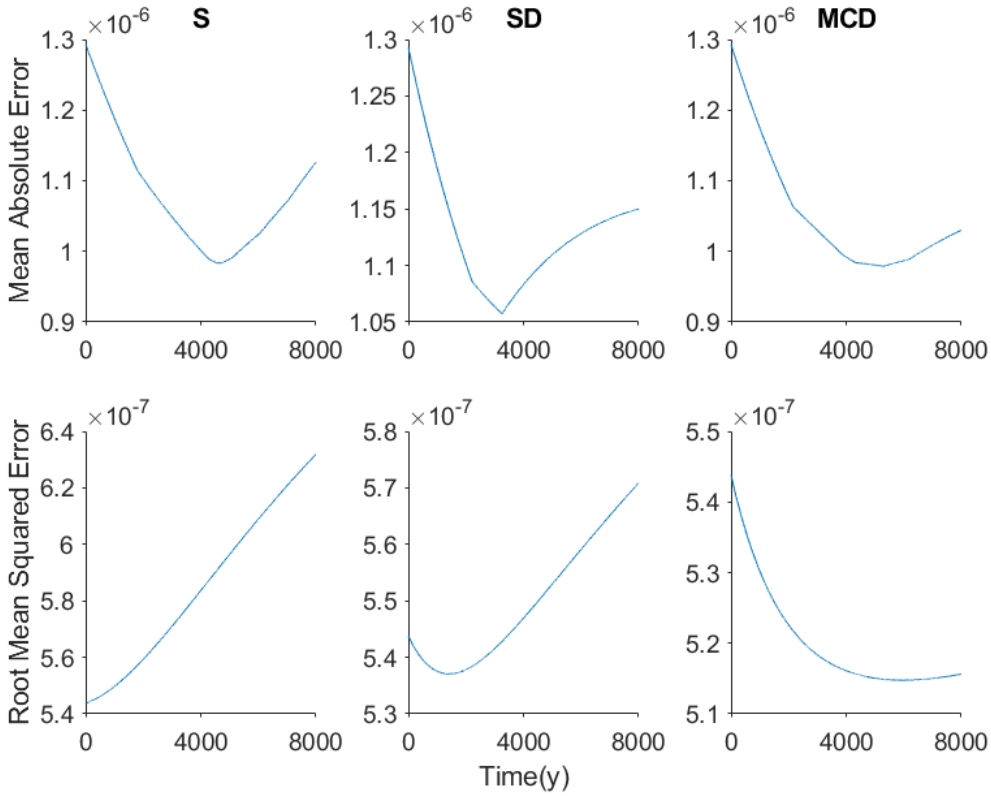

Figure 3.9: The mean differences between Powell Lake's measurements and our three approaches.

after 5000 years to the initial concentration, with the actual chemical composition of the relic seawater on the bottom of the lake. To show what drives the differences seen in these 3 approaches of the diffusion of salt we compare also the diffusivities that apply to our 3 simulations.

In order to calculate the relative difference between the values of our three approaches after 5000 years and the measured values in Powell Lake we use the following formula:

$$\%Difference = \frac{MCD_i - P_i}{P_i} \times 100 \tag{3.11}$$

where MCD_i is the value with the MCD approach for each ion and P_i is the mea-

sured value in Powell Lake. We use the same formula to calculate the differences between the Simple Diffusion and Single Salt cases.

Calculating the difference of the three approaches to Powell Lake's ratios (table 3.3), we notice that for all of the ions, except potassium, the MCD approach reaches values that are closer to the measured values for the present-day lake's chemical composition than Simple Diffusion. The Single Salt approach also seems to be quite accurate for magnesium, potassium and strontium but MCD is more accurate for ions that form a much greater amount of the salt content of seawater.

We also calculate the weighted average of the differences for the MCD, SD and Single Salt cases in order to more objectivelly show which one is a better match with Powell Lake's measurements:

$$W_{MCD} = \frac{\sum [\%]_{sea}[\%]_{MCD}}{\sum [\%]_{sea}} \tag{3.12}$$

where $[\%]_{sea}$ is the percentage of sea salt that each ion forms and $[\%]_{MCD}$ is the percentage difference shown in table 3.3 for the MCD approach. Similarly, we calculate the weighted average for the Simple Diffusion and Single Salt approach. The result is that the average difference of the Powell Lake's measurements with the MCD approach is 6.3% while with the Single Salt approach the difference is 6.9% and with the Simple Diffusion case is 42.4%.

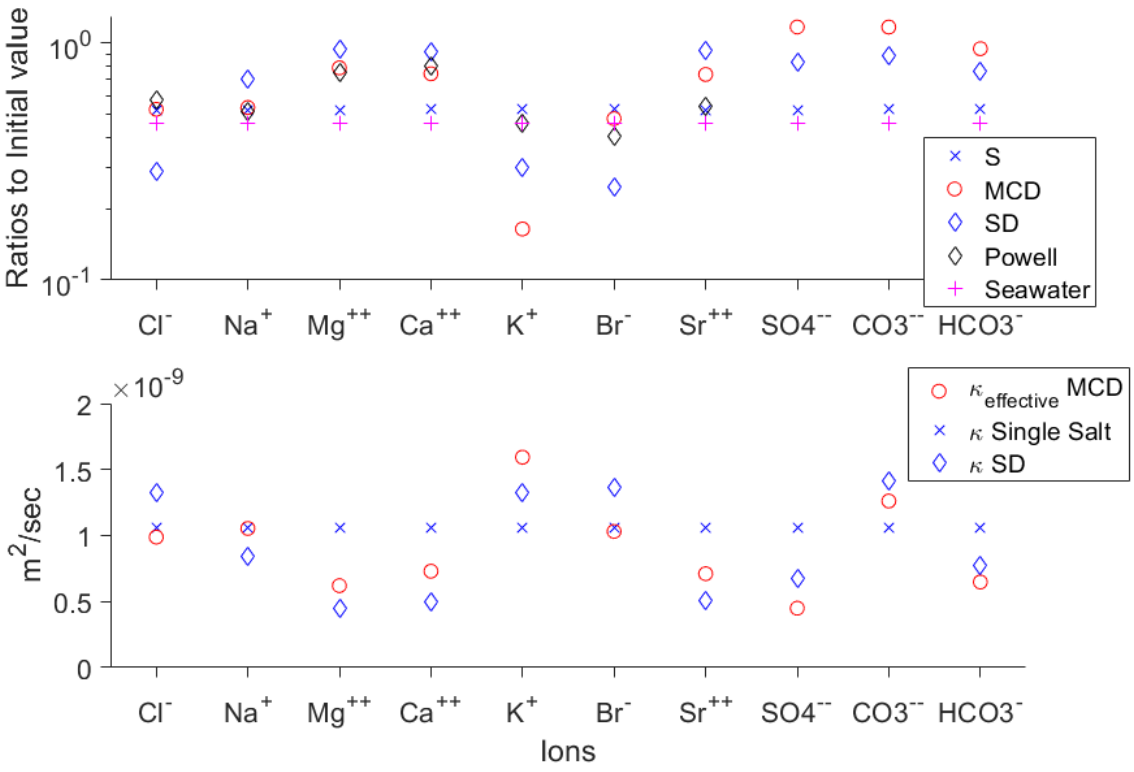

Figure 3.10: a) Comparison of ratios of MCD, SD, single salt diffusion, Powell Lake observations and seawater ratios from a salinity 35g/kg to 16 as it happened in the lake. The Powell Lake's ratios for sulfates are not appearing because the ratio is very small in the order of 10^{-3} and the carbonate and bicarbonate are in the order of 1. b) The diffusivities for MCD, SD and single salt ($NaCl$).

Table 3.2: The specific diffusivity calculated for each ion using the Nernst equation Li and Gregory (1973) for the lake's temperature at approximately 9°C

Ion characteristics for our model		
Ion	Charge number	Diffusivity (10^{-9} m^2/s)
Cl^-	-1	1.3347
Na^+	+1	0.8552
Mg^{2+}	+2	0.45
Ca^{2+}	+2	0.5
K^+	+1	1.3051
Br^-	-1	1.3808
Sr^{2+}	+2	0.255
SO_4^{2-}	-2	0.341
CO_3^{2-}	-2	0.306
HCO_3^-	-1	0.7893

Table 3.3: The relative difference for the three approaches with Powell Lake's values for the three approaches

Ion	MCD	SD	S
Cl^-	-8.3%	-50.1%	-8.9%
Na^+	2.8%	36.2%	0.98%
Mg^{2+}	4.1%	25.5%	-30%
Ca^{2+}	-6.6%	15.5%	-33.5%
K^+	-64.1%	-34.4%	14.6%
Br^-	19.1%	-38.5%	30.1%
Sr^{2+}	36.4%	71.38%	-3.6%

Chapter 4

Discussion

Double Diffusion (DD) is a mechanism that has been identified in many regions of the ocean and in lakes such as Powell Lake (Carpenter and Timmermans, 2012). The unique staircases that double diffusion creates in the vertical temperature and salinity profiles have been investigated by researchers who studied double diffusion using observations and simple diffusion models (Radko, 2013; Carpenter et al., 2012a,b; Carpenter and Timmermans, 2014; Sanderson et al., 1986). However, all of this work has treated sea salt as a single substance with a fixed diffusivity. In reality, sea salt is a complex mixture of constituents, and multicomponent diffusion effects occur although their importance is yet unknown. The present work is a first attempt to quantify the effect of multicomponent diffusion on the transport of salt in seawater. We use Powell Lake as an analogue to simulate a step and extend our knowledge regarding this process.

4.1 Implications for Powell Lake

The salinity of seawater depends mostly on the concentration of 10 major ions. These ions have different diffusion rates through a staircase, and using a numerical simulation we have estimated what these differences are. In our simulation all ions diffuse from the higher salinity region to the lower one following an error function-type curvature. Sulfate also diffuses in this direction but its profile also includes a slight minimum and maximum.

Different behaviour of sulfate relative to other ions has also been noticed in investigations of the Soret effect in seawater by Caldwell and Eide (1985a). They speculate that a multicomponent effect may be occuring, implying ion/ion electric field interaction, but make no further analysis. Their dataset was not comprehensive enough to find whether potassium diffusion was larger than expected as we have found. Ions at low concentrations have been found to have anomalous behaviour in other cases as well (Rasouli et al., 2015).

From eq. 3.4 we see that the total flux for each ion will be the sum of its diffusive flux affected by the chemical gradient and its electrical potential driven flux affected by the electrical potential. Cations appear to have greater diffusion rates due to the effect of the electrical potential while anions are slowed down with changes of O(15-25%) in the effective diffusivity (fig. 3.5).

Comparing our multicomponent diffusion approach for long-term changes with the approaches that treat the salt content of seawater as a single salt where all ions have the same diffusivity, or as a simple diffusive system where all ions have different diffusivities but we ignore the effect of electrical potential (fig. 3.7), we find that MCD provides the best match to the ratios seen in present-day Powell Lake seawater (fig. 3.10 and table 3.3) but improvement for the Single Salt approach is only marginal. However, differences remain, with K^+/Cl^- ratios being the greatest one, and these may be due to the effect of other geochemical processes.

There are three major sources of salts in typical lakes. Lakes get airborne salts from the exchange with the atmosphere, salts derived from weathering of the soils and rocks and from river input and underground sources.

The weathering of the rocks and sediments is the most important source of salts in lakes whether fresh or saline (Fuller, 1974). The decomposition of the rocks into sediments which will then become soils will lead to the availability of minerals for the lake's chemical composition (Rutherford and Sullivan, 1970). Ruttner and Ruttner-Kolisko (1972) investigated the origin of salts and discuss that Paleozoic shales, sandstones and evaporites can carry salts in a very short time. When a lake's ionic ratios are controlled by rock dominant processes then the lake is expected to be rich in calcium (Kilham, 1990) and bicarbonate differences are probably due to the decomposition of organic material. This is why in fig.3.10 we see the Powell Lake observations to be higher for these ions than the estimated ones. Following

Gibbs (1970) and Stallard (1980) we can expect that in Powell Lake the ionic ratios that are set by the seawater source can be affected by rock processes that may be affecting the chemical composition of the lake.

The role of the atmosphere in the concentration of salts in lakes is also very important. The cyclic salts theory claims that salts from the ocean are carried by the wind as droplets or dry particles inland and are subsequently precipitated in rain. Rain contains sodium, calcium and potassium among other salts (Junge and Werby, 1958). Thus, salts are accumulating in lakes (Anderson, 1945). Johnson (1980) continues this theory and states that the amount of salt depends on the distance that the lake has from the sea and the wind force. This theory could explain the higher values of potassium from fig. 3.10.

Eugster and Jones (1979) conclude that the chemical fractionation that takes place in closed basins is accounted for by mineral precipitation and sediment coatings, sorption on active surfaces, degassing and redox reactions. Major ions are differently affected by each process and may differ from basin to basin. Sodium and magnesium could be decreased by exchange processes on active surfaces and this would explain the lower values in fig. 3.10.

4.2 Implications for the Ocean

The double diffusive staircases that we investigated in Powell Lake also appear in various regions of the global ocean and in the Arctic. Timmermans et al. (2003) described a staircase in the deep waters of the Arctic Ocean in the Canada Basin. The staircase appears in depths of 2400-2800 m where the water mases are trapped under the sill depth of the Alpha-Mendeleyev ridge complex. The deeper trapped waters are estimated by a ^{14}C isolation age estimate to be between 450 and 1000 years old (Macdonald and Carmack, 1991; Timmermans et al., 2003; Schlosser et al., 1997).

Multicomponent diffusion may be the main transport mechanism in this area of the ocean affecting the exchange of deep waters with those above. If true, then simulating this mechanism we can see that there is a slow change in the relative composition of salt above and below the interface with time (fig. 3.7). Each ion has a different diffusivity and therefore its loss rate is different than the other ions.

Table 4.1: Ratios of ions to Cl^- from the study of Millero et al. (2008) and comparison of the digits of significance with MCD changes after 500y and 1000y

Ions	Ratios to Cl^- at S=35g/kg	Difference after 500y (% change)	Difference after 1000y (% change)
Na^+	0.557	+0.001(0.1%)	+0.003(0.3%)
Mg^{2+}	0.066	+0.004(4.1%)	+0.008(8.3%)
Ca^{2+}	0.021	+0.0006(3.5%)	+0.001(7.1%)
K^+	0.0205	-0.002(10.9%)	-0.004(20.7%)
Br^-	0.0035	-0.00001(0.9%)	-0.00002(1.8%)
Sr^{2+}	0.0004	+0.000005(3.4%)	+0.00001(7%)
SO_4^{2-}	0.14	+0.004(8.3%)	+0.009(17.3%)

If this is also the case in the Arctic, the different diffusivity of the ions affects the chemical composition of seawater by changing the ratios of the ions present in seawater.

We calculate MCD-induced changes in the ratios of the ions to Cl^- in the deep Canada basin after 500 and 1000 years (table 4.1). We find the ratios to be increasing with time for most of the ions except potassium and bromine where the ratios are decreasing. The reason is that the effective diffusivities of Br^- and K^+ are greater than Cl^- and therefore these two ions diffuse faster than Cl^-. For the estimation of the ratios of the ions in a chemistry laboratory a typical accuracy is 2% (American Public Health Association et al., 1995). Most of the changes we predict exceed this value. Thus the results of MCD, if they controlled exchange, would be measurable. However, we are not aware of any major ion composition measurements to resolve this speculation.

4.3 Modelling the Diffusivity of Salt

The salt in seawater is a mixture of dissolved ions that exist in different concentrations. The ratios of the ions to each other are known to be quite stable, although no major ion composition measurements have been made in the Arctic (Culkin and Cox, 1966; Carpenter and Manella, 1973; Riley and Tongudai, 1967; Morris and Riley, 1966).

In the current literature researchers have been addressing the diffusivity of salt as a constant parameter when studying diffusive effects (Stern, 1960; Radko, 2013; Zaloga, 2015; Scheifele, 2013; Carpenter et al., 2012a,b; Carpenter and Timmermans, 2014). Our study shows that the ions that form the salt content of seawater have different diffusivities and therefore diffuse at different rates. This leads to a noticable change in the chemical composition of seawater with time. In areas where turbulent mixing occurs, the time scales would not allow diffusion to make important changes to the concentration of the ions. But in areas where water is not affected by turbulent mixing or currents, MCD may be an important force. Salt's diffusivity should be considered as a separate parameter for each ion when studying the behaviour of separate ions.

In the ocean, the instability scales are defined based on specific ranges of the density ratio (Radko, 2013). This range depends on the Prandtl number (Pr) (which is defined as the ratio of kinematic viscosity to thermal diffusivity) which in the ocean is Pr≈6 (Radko, 2013; Scheifele, 2013; Haigh, 1995) for T=25°C and on the ratio (τ) of the thermal diffusivity to the diffusivity of salt.

$$1 < R_\rho < \frac{Pr+1}{Pr+\tau} \tag{4.1}$$

The thermal diffusivity is 1.4×10^{-7} m^2s^{-1} Radko (2013) while the diffusivity of salt has long been considered as a constant value for single salt diffusivity for different studies (1.1×10^{-9} m^2s^{-1} (Radko, 2013) for any temperature and 1.3×10^{-9} m^2s^{-1} (Stern, 1960) for T=20°C) but this should not be the case.

What value should we use? One option is to see that MCD tends to make Na^+ and Cl^- diffuse at nearly the same rate. In the absense of other ions, electric fields would make them diffuse exactly the same rate, so $NaCl$ is a useful model for seawater. An alternative is to form a weighted average:

$$\bar{\kappa} = \frac{\sum c_i \kappa_{eff}}{\sum c_i} \tag{4.2}$$

which gives values that have a difference with the first option by 5-7% over a range of temperatures from 1 to 26°C. In either case, we can now provide an estimate of how salt's diffusivity varies with temperature.

Table 4.2: Temperature (T) dependence of Salt's diffusivity (D)

T (°C)	D (10^{-9} m^2/s)	T (°C)	D (10^{-9} m^2/s)
1	0.81	14	1.20
2	0.83	15	1.24
3	0.86	16	1.27
4	0.89	17	1.30
5	0.92	18	1.34
6	0.95	19	1.38
7	0.98	20	1.41
8	1.01	21	1.45
9	1.04	22	1.49
10	1.07	23	1.53
11	1.10	24	1.57
12	1.13	25	1.61
13	1.17	26	1.64

4.4 Conclusion

Using MIN3P it is possible to simulate the steps and chemical compositions of the areas of the ocean where the staircase appears, in order to assist any ongoing investigation. However, in our calculations we do not include other chemical or physical reactions that could affect the chemical composition of seawater and we are simulating one step with specific characteristics. Simulations for the specific steps and eventually the whole staircase at areas where double diffusion is noticed, are important to maximize the accuracy of our results.

The diffusivity of salt used for the estimation of instabilities in the ocean has proven to be valid even with the effect of a multicomponent system. However, when modelling the diffusivity of salt the effect of temperature should be taken into account.

Changes in the chemical composition of seawater could affect the physical, chemical and biological properties of seawater and in areas where Double Diffusion appears the chemistry of seawater will change with time. We suggest that researchers interested in the chemistry of seawater should consider the effect of MCD to the chemical composition of seawater, for timescales longer than 500 years, in areas such as the Canada Basin in the Arctic Ocean where water ages

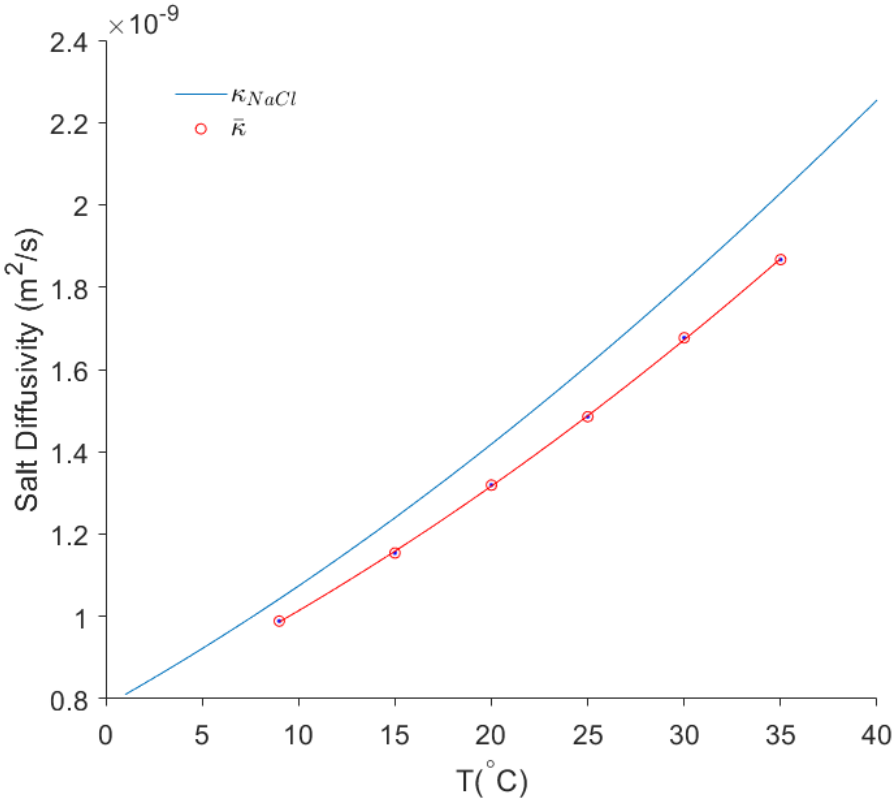

Figure 4.1: The temperature effect on Salt's Diffusivity

without turbulent mixing present.

Bibliography

American Public Health Association, A. et al. (1995). *Standard methods for the examination of water and wastewater*, Volume 21. American public health association Washington, DC. → page 41

Anderson, V. G. (1945). Some effects of atmospheric evaporation and transpiration on the composition of natural waters in Australia. *J. Proc. Aust. chem. Inst 12*, 40–68. → page 40

Balistrieri, L. and J. Murray (1982). The adsorption of cu, pb, zn, and cd on goethite from major ion seawater. *Geochimica et cosmochimica acta 46*(7), 1253–1265.

Balluffi, R. W., S. Allen, and W. C. Carter (2005). *Kinetics of materials*. John Wiley & Sons. → page 12

Boudreau, B. P. (1997). *Diagenetic models and their implementation*, Volume 505. Springer Berlin. → page 17

Bouty, E. (1880). Ch. soret.—sur l'état d'équilibre que prend, au point de vue de sa concentration, une dissolution saline primitivement homogène, dont deux parties sont portées à des températures différentes; archives de genève, 3e periode, t. ii, p. 48; 1879. *J. Phys. Theor. Appl. 9*(1), 331–332. → page 13

Caldwell, D. and S. Eide (1985a). Separation of seawater by soret diffusion. *Deep Sea Research Part A. Oceanographic Research Papers 32*(8), 965–982. → pages 13, 15, 16, 17, 39

Caldwell, D. R. and S. A. Eide (1985b). Separation of seawater by Soret diffusion. *Deep Sea Research Part A, Oceanographic Research Papers 32*(8), 965–982. → pages 13, 14

Carpenter, J. and M. Manella (1973). Magnesium to chlorinity ratios in seawater. *Journal of Geophysical Research 78*(18), 3621–3626. → page 41

Carpenter, J., T. Sommer, and A. Wüest (2012a). Simulations of a double-diffusive interface in the diffusive convection regime. *Journal of Fluid Mechanics 711*, 411–436. → pages 38, 42

Carpenter, J., T. Sommer, and A. Wüest (2012b). Stability of a double-diffusive interface in the diffusive convection regime. *Journal of Physical Oceanography 42*(5), 840–854. → pages 38, 42

Carpenter, J. and M.-L. Timmermans (2014). Does rotation influence double-diffusive fluxes in polar oceans? *Journal of Physical Oceanography 44*(1), 289–296. → pages 38, 42

Carpenter, J. R. and M.-L. Timmermans (2012). Temperature steps in salty seas. *Physics Today 65*(3), 66–67. → pages 2, 38

Clague, J. J. and T. S. James (2002). History and isostatic effects of the last ice sheet in southern british columbia. *Quaternary Science Reviews 21*(1-3), 71–87. → page 20

Culkin, F. and R. Cox (1966). Sodium, potassium, magnesium, calcium and strontium in sea water. In *Deep Sea Research and Oceanographic Abstracts*, Volume 13, pp. 789–804. Elsevier. → page 41

Cussler, E. L. (2009). *Diffusion: mass transfer in fluid systems*. Cambridge university press. → page 17

Davies, C. W. and T. Shedlovsky (1964). Ion association. *Journal of The Electrochemical Society 111*(3), 85C—-86C. → page 60

Debye, P. (1923). The theory of electrolytes I. The lowering of the freezing point and related occurrences. *Physikalische Zeitschrift 24*, 185–206. → page 60

Dickinson, E. J., J. G. Limon-Petersen, and R. G. Compton (2011). The electroneutrality approximation in electrochemistry. *Journal of Solid State Electrochemistry 15*(7-8), 1335–1345. → page 14

Easley, R. A. and R. H. Byrne (2012). Spectrophotometric calibration of ph electrodes in seawater using purified m-cresol purple. *Environmental science & technology 46*(9), 5018–5024. → pages 15, 17

Eugster, H. P. and B. F. Jones (1979). Behavior of major solutes during closed-basin brine evolution. *American journal of science 279*(6), 609–631. → page 40

Felmy, A. R. and J. H. Weare (1991). Calculation of multicomponent ionic diffusion from zero to high concentration: II. Inclusion of associated ion species. *Geochimica et Cosmochimica Acta 55*(1), 133–144. → page 11

Fuller, W. H. (1974). Desert soils. *Desert Biology: Special Topics on the Physical and Biological Aspects of Arid Regions 2*, 31–102. → page 39

Giambalvo, E. R., C. I. Steefel, A. T. Fisher, N. D. Rosenberg, and C. G. Wheat (2002). Effect of fluid-sediment reaction on hydrothermal fluxes of major elements, eastern flank of the juan de fuca ridge. *Geochimica et Cosmochimica Acta 66*(10), 1739–1757. → pages 16, 17

Gibbs, R. J. (1970). Mechanisms controlling world water chemistry. *Science 170*(3962), 1088–1090. → page 40

Haigh, S. P. (1995). *the faculty of graduate studies department of mathematics institute of applied mathematics*. Ph. D. thesis, university of british columbia. → page 42

Horne, R. (1969). Marine chemistry, 568 pp. *Inter-science, New York*. → page 1

Hyndman, R. D. (1976). Heat flow measurements in the inlets of southwestern British Columbia. *Journal of Geophysical Research 81*(2), 337–349. → page 20

Johannesson, B., K. Yamada, L.-O. Nilsson, and Y. Hosokawa (2007). Multispecies ionic diffusion in concrete with account to interaction between ions in the pore solution and the cement hydrates. *Materials and Structures 40*(7), 651. → page 17

Johnson, J. K. (1980). Effects of temperature and salinity on production and hatching of dormant eggs of Acartia californiensis (Copepoda) in an Oregon estuary. *Fish. Bull 77*(3), 567–584. → page 40

Jost, W. (1960). *Diffusion in Solids, Liquids, Gases: 3d Print., with Addendum*. Academic Press. → pages 12, 28

Junge, C. E. and R. Werby (1958). The concentration of chloride, sodium, potassium, calcium, and sulfate in rain water over the united states. *Journal of Meteorology 15*(5), 417–425. → page 40

Kang, Q., P. C. Lichtner, and D. Zhang (2006). Lattice boltzmann pore-scale model for multicomponent reactive transport in porous media. *Journal of Geophysical Research: Solid Earth 111*(B5). → page 17

Kelley, D. E., H. J. Fernando, A. E. Gargett, J. Tanny, and E. Özsoy (2003). *The diffusive regime of double-diffusive convection*. Ph. D. thesis. → pages 2, 6

Kennish, M. J. (2000). *Practical handbook of marine science*. crc press. → page 1

Kilham, P. (1990). Mechanisms controlling the chemical composition of lakes and rivers: Data from Africa. *Limnology and Oceanography 35*(1), 80–83. → page 39

Lasaga, A. C. (1979). *Multicomponent exchange and diffusion in silicates*. Ph. D. thesis. → pages 11, 12

Lasaga, A. C. (1998). Kinetic Theory in the Earth SciencesPrinceton Univ. *Press, Princeton, NJ*. → pages 11, 12, 16, 17

Li, Y. H. and S. Gregory (1973). diffusion of ions in seawater and deep sea sediments, submitted to Geochim. *Cosmochim. Acta*. → pages ix, x, x, 8, 12, 23, 24, 28, 37

Macdonald, R. and E. Carmack (1991). Age of canada basin deep waters: a way to estimate primary production for the arctic ocean. *Science 254*(5036), 1348–1350. → page 40

MacQuarrie, K. T. and K. U. Mayer (2005). Reactive transport modeling in fractured rock: A state-of-the-science review. *Earth-Science Reviews 72*(3-4), 189–227.

Marcet, A. J. G. (1819). Xii. on the specific gravity, and temperature of sea waters, in different parts of the ocean, and in particular seas; with some account of their saline contents. *Philosophical Transactions of the Royal Society of London* (109), 161–208. → page 1

Mathews, W. H. (1962). *Bathymetry of Powell Lake, British Columbia*. Institute of Oceanography, University of British Columbia. → page 20

Mathews, W. H., J. G. Fyles, and H. W. Nasmith (1970). Postglacial crustal movements in southwestern British Columbia and adjacent Washington State. *Canadian Journal of Earth Sciences 7*(2), 690–702. → pages 9, 20

Mayer, K. U., E. O. Frind, and D. W. Blowes (2002). *Multicomponent reactive transport modeling in variably saturated porous media using a generalized formulation for kinetically controlled reactions*. Ph. D. thesis. → page 18

Millero, F. J. (2001). *The physical chemistry of natural waters*, Volume 2. Wiley-Interscience New York. → page 59

Millero, F. J. (2016). *Chemical oceanography*. CRC press. → page 1

Millero, F. J., R. Feistel, D. G. Wright, and T. J. McDougall (2008). The composition of standard seawater and the definition of the reference-composition salinity scale. *Deep Sea Research Part I: Oceanographic Research Papers 55*(1), 50–72. → pages ix, 22, 41

Morris, A. W. and J. Riley (1966). The bromide/chlorinity and sulphate/chlorinity ratio in sea water. In *Deep sea research and oceanographic Abstracts*, Volume 13, pp. 699–705. Elsevier. → page 41

Muniruzzaman, M., C. M. Haberer, P. Grathwohl, and M. Rolle (2014). Multicomponent ionic dispersion during transport of electrolytes in heterogeneous porous media: Experiments and model-based interpretation. *Geochimica et Cosmochimica Acta 141*, 656–669. → pages 16, 17

Murray, J. W., Z. Top, and E. Özsoy (1991). Hydrographic properties and ventilation of the black sea. *Deep Sea Research Part A. Oceanographic Research Papers 38*, S663–S689. → page 1

Oelkers, E. H. (1996). Physical and chemical properties of rocks and fluids for chemical mass transport calculations. In *Reactive transport in porous media*, Volume 34, pp. 131–191. MINERALOGICAL SOC AMERICA. → pages 11, 12

Osborn, T. R. (1973). Temperature microstructure in Powell Lake. *Journal of Physical Oceanography 3*(3), 302–307. → page 19

Padman, L. and T. M. Dillon (1989). *Thermal microstructure and internal waves in the Canada Basin diffusive staircase*. Ph. D. thesis. → page 2

Parkhurst, D. L., C. Appelo, et al. (1999). User's guide to phreeqc (version 2): A computer program for speciation, batch-reaction, one-dimensional transport, and inverse geochemical calculations. *Water-resources investigations report 99*(4259), 312. → pages 17, 60

Pawlowicz, R. (2008). Calculating the conductivity of natural waters. *Limnology and Oceanography: Methods 6*(9), 489–501. → page 22

Paz-García, J. M., B. Johannesson, L. M. Ottosen, A. B. Ribeiro, and J. M. Rodríguez-Maroto (2011). Modeling of electrokinetic processes by finite element integration of the nernst–planck–poisson system of equations. *Separation and Purification Technology 79*(2), 183–192. → page 17

Perry, K. A. and T. F. Pedersen (1993). Sulphur speciation and pyrite formation in meromictic ex-fjords. *Geochimica et Cosmochimica Acta 57*(18), 4405–4418. → pages 20, 22

Pitzer, K. S. (1991). Ion interaction approach: theory and data correlation. *Activity coefficients in electrolyte solutions 2*, 75–153. → page 61

Poling, B. E., J. M. Prausnitz, J. P. O'connell, et al. (2001). *The properties of gases and liquids*, Volume 5. Mcgraw-hill New York. → page 29

Radko, T. (2013). *Double-diffusive convection*. Cambridge University Press. → pages 38, 42

Rasouli, P., C. I. Steefel, K. U. Mayer, and M. Rolle (2015). Benchmarks for multicomponent diffusion and electrochemical migration. *Computational Geosciences 19*(3), 523–533. → pages 16, 18, 24, 39

Reinhardt, K. and W. Kern (2018). *Handbook of silicon wafer cleaning technology*. William Andrew. → page 13

Riley, J. and M. Tongudai (1967). The major cation/chlorinity ratios in sea water. *Chemical Geology 2*, 263–269. → page 41

Robinson, R. A. (1959). Stokes, RH Electrolyte Solutions. *London, Butterworths Scientific Publications 19550*(2), 540–544. → page 12

Rolle, M., M. Muniruzzaman, C. M. Haberer, and P. Grathwohl (2013). Coulombic effects in advection-dominated transport of electrolytes in porous media: Multicomponent ionic dispersion. *Geochimica et Cosmochimica Acta 120*, 195–205. → page 24

Ruddick, B. and A. E. Gargett (2003). Oceanic double-infusion: Introduction. *Progress in Oceanography 56*(3-4), 381–393. → page 2

Rutherford, G. K. and D. K. Sullivan (1970). Properties and geomorphic relationships of soils developed on a quartzite ridge near Kingston, Ontario. *Canadian Journal of Soil Science 50*(3), 419–429. → page 39

Ruttner, A. W. and A. E. Ruttner-Kolisko (1972). Some data on the hydrology of the Tabas-Shirgesht-Ozbak-kuh area (East Iran). *Jahrbuch der Geologischen Bundesanstalt, Wien 115*, 1–48. → page 39

Sanderson, B., K. Perry, and T. Pedersen (1986). Vertical diffusion in meromictic Powell lake, British Columbia. *Journal of Geophysical Research: Oceans 91*(C6), 7647–7655. → pages 9, 19, 20, 38

Scheifele, B. (2013). Scheifele, B.: Double Diffusion in Powell Lake. (September). → pages x, x, x, 2, 3, 5, 17, 20, 21, 31, 42

Scheifele, B., R. Pawlowicz, T. Sommer, and A. Wüest (2014). Double Diffusion in Saline Powell Lake, British Columbia. *Journal of Physical Oceanography 44*(11), 2893–2908. → pages 9, 19

Schlosser, P., B. Kromer, B. Ekwurzel, G. Bönisch, A. McNichol, R. Schneider, K. Von Reden, H. Östlund, and J. Swift (1997). The first trans-arctic 14c section: comparison of the mean ages of the deep waters in the eurasian and canadian basins of the arctic ocean. *Nuclear Instruments and Methods in Physics Research Section B: Beam Interactions with Materials and Atoms 123*(1-4), 431–437. → page 40

Schmitt, R. (2002). Double Diffusion in Oceanography. *Annual Review of Fluid Mechanics 26*(1), 255–285. → page 3

Schmitt, R. W. (1994). Double diffusion in oceanography. *Annual Review of Fluid Mechanics 26*(1), 255–285. → page 6

Shiba, S., Y. Hirata, and T. Seno (2005). Mathematical model for hydraulically aided electrokinetic remediation of aquifer and removal of nonanionic copper. *Engineering geology 77*(3-4), 305–315. → pages 16, 17

Stallard, R. F. (1980). *Major element geochemistry of the Amazon River system*. Ph. D. thesis, Massachusetts Institute of Technology. → page 40

Steefel, C. I., S. Carroll, P. Zhao, and S. Roberts (2003). Cesium migration in hanford sediment: a multisite cation exchange model based on laboratory transport experiments. *Journal of Contaminant Hydrology 67*(1-4), 219–246. → page 17

Stern, M. E. (1960). The "salt-fountain" and thermohaline convection. *Tellus 12*(2), 172–175. → pages 6, 42

Stommel, H. (1956). An oceanographic curiosity: the perpetual salt fountain. *Deep-Sea Res. 3*, 152–153. → page 5

Thurman, H. V. and E. A. Burton (1997). *Introductory oceanography*. Prentice Hall New York. → page 1

Timmermans, M.-L., C. Garrett, and E. Carmack (2003). The thermohaline structure and evolution of the deep waters in the canada basin, arctic ocean. *Deep Sea Research Part I: Oceanographic Research Papers 50*(10-11), 1305–1321. → pages 1, 3, 40

Turner, J. (1969). A physical interpretation of the observations of hot brine layers in the red sea. In *Hot brines and recent heavy metal deposits in the Red Sea*, pp. 164–173. Springer. → page 14

Wang, Y. and P. Van Cappellen (1996). A multicomponent reactive transport model of early diagenesis: Application to redox cycling in coastal marine sediments. *Geochimica et Cosmochimica Acta 60*(16), 2993–3014. → page 17

Williams, P. M., W. H. Mathews, and G. L. Pickard (1961). A lake in British Columbia containing old sea-water. *Nature 191*(4790), 830. → page 20

Wright, M. R. (2007). *An introduction to aqueous electrolyte solutions*. John Wiley & Sons. → page 59

Zaloga, A. (2015). *Spatial and temporal variability of double diffusive structures in Powell Lake, British Columbia*. Ph. D. thesis, University of British Columbia. → pages 3, 7, 42

Appendix A

MIN3P Input Files

In order to run MIN3P there are two files that we will be changing. One is the input file (.dat) and the other is the database file (.dbs). The structure of the input file (.dat) that we set for our approach is divided into sections or data blocks. Each data block contains specific input information and is bounded by a keyword at the top and a 'done' statement at the end. There is a total of 17 data blocks but most of them remain in default for our simulation because they contain general control parameters so we will discuss only the most important ones.

A.1 Data Block 1: Global Control Parameters

In this the first data block we set MIN3P's extension as a multicomponent diffusion model.

A.2 Data Block 2: Geochemical System

In the second data block we set the Pitzer equations and the database that links each ion to its own diffusivity, previous calculated using the Nernst equation (table3.2) which is stored in the database file in the MCD database directory. We also set the number and name of the ions that will be used in the following steps as well as the units for their concentrations that are set in Data Block 14.

```
! Data Block 1: global control parameters
! ------------------------------------------------------------------------------
!
'global control parameters'
'Multicomponent Diffusion Test'
.true.                          ;varsat_flow
.true.                          ;steady_flow
.true.                          ;fully_saturated
.true.                          ;reactive_transport


'multicomponent diffusion'
'done'
```

Figure A.1: Data Block 1

```
! Data Block 2: geochemical system
! ------------------------------------------------------------------------------
!
'geochemical system'

'use new database format'

'database directory'
'MCD'

'define input units'
'mol/l'

'components'
10                              ;number of components (nc-1)
'cl-1'
'na+1'
'mg+2'
'ca+2'
'k+1'
'br-1'
'sr+2'
'so4-2'
'co3-2'
'hco3-'

'done'
```

Figure A.2: Data Block 2

A.3 Data Block 3: Spatial Discretization

In the third data block we set the two regions of our model which means that we set an upper layer and its x,y,z dimensions and a lower layer and its x,y,z dimensions as well as the grid points for each area. When simulating the diffusive step we use more grid points close to the interface in order to get smoother curvatures.

```
! Data Block 3: spatial discretization
! ------------------------------------------------------------------------
!
'spatial discretization'
1                              ;number of discretization intervals in x
1                              ;number of control volumes in x
0. 1.0                         ;xmin,xmax
1                              ;number of discretization intervals in y
1                              ;number of control volumes in y
0. 1.0                         ;ymin,ymax
3                              ;number of discretization intervals in z
500                            ;number of control volumes in z
0. 290.0                       ;zmin,zmax
1000                           ;number of control volumes in z
290.0 310.0                    ;zmin,zmax
500                            ;number of control volumes in z
310.0 320.0                    ;zmin,zmax

'done'
```

Figure A.3: Data Block 3

```
! Data Block 4: time step control - global system
! ------------------------------------------------------------------
!
'time step control - global system'
'hours'                        ;time unit
0.0                            ;time at start of solution
10.0                           ;final solution time
1.0                            ;maximum time step
3.0d-4                         ;minimum time step


'done'
```

Figure A.4: Data Block 4

A.4 Data Block 4: Time Step Control

In the fourth data block we set the time units, the time step and the initial and final solution time. We set the final solution time to 10 hours for the reasons discussed earlier.

A.5 Data Block 8: Output Control

In this data block we set the spatial output of data from our simulation which could be several specified times between 0 and 10 hours if we want to see the evolution of our system.

```
! Data Block 8: output control
! ------------------------------------------------------------------------------
!
'output control'

'output activity coefficients'

'output of spatial data'
1                              ;number of output times (spatial data)
10                 ;specified output times (spatial data)


'output of transient data'
3                              ;number of output locations (transient data)
1                              ;timesteps between output (transient data)
1 2 3                             ;control volume numbers for transient data

'done'
```

Figure A.5: Data Block 8

```
! Data Block 11: physical parameters - reactive transport
! ------------------------------------------------------------------------------
!
'physical parameters - reactive transport'

'diffusion coefficients'
2.0d-9                         ;aqueous phase
```

Figure A.6: Data Block 11

A.6 Data Block 11: Physical Parameters - Reactive Transport

This data block will be inactive in the multicomponent diffusion approach but it becomes important for the cases of simple diffusion where we set the diffusivity for each ion and single salt diffusion where we set a global diffusion coefficient for our solution.

A.7 Data Block 14: Initial Condition - Reactive Transport

In this data block we set the initial conditions at the two regions of our simulation. The data block is divided into two zones where the first one is being set by us to be the upper layer and it contains the concentration input for each ion as well as the statement 'charge' for chloride which will control the charge balance of the

```
! Data Block 14: initial condition - reactive transport
! ------------------------------------------------------------------
!
'initial condition - reactive transport'
2                              ;number of zones

! ------------------------------------------------------------------
'number and name of zone'
1
'background chemistry - upper part with S=35'


'concentration input'
0.5462 'charge' ;'cl-1'
0.4692 'free' ;'na+1'
0.0528 'free' ;'mg+2'
0.0103 'free' ;'ca+2'
0.0102 'free' ;'k+1'
8.42e-4 'free' ;'br-1'
9.06e-5 'free' ;'sr+2'
0.0282 'free' ;'so4-2'
0.0017 'free' ;'co3-2'
2.39e-4 'free' ; 'hco3-'




'extent of zone'
0.0 1.0  0.0 1.0  300.0 320.0

'end of zone'
```

Figure A.7: Data Block 14a

solution. We also specify the extent of the zone and name it. The second zone similar to the first one contains the concentration input for the lower layer and we also set the 'charge' statement for chloride and the extent of the zone. In this study we consider the carbonate and bicarbonate ions decoupled.

A.8 Data Block 16: Boundary Conditions - Reactive Transport

In this block we can specify the boundary conditions of our model. Since we do not need some specific boundary conditions we leave this block to 'default' for all of our simulations which means that the boundary conditions will be the initial conditions.

```
'number and name of zone'
2
'background chemistry - lower part with S=0.00001'

'concentration input'
1.56e-07 'charge' ;'cl-1'
1.34e-07 'free' ;'na+1'
1.5e-08 'free' ;'mg+2'
2.93e-09 'free' ;'ca+2'
2.91e-09 'free' ;'k+1'
2.4e-10 'free' ;'br-1'
2.5e-11 'free' ;'sr+2'
8e-09 'free' ;'so4-2'
4.9e-10 'free' ;'co3-2'
6.8e-11 'free' ; 'hco3-'



'extent of zone'
0.0 1.0  0.0 1.0  0.0 300.0

'end of zone'
'done'
```

Figure A.8: Data Block 14b

```
1  hco3-      -1.0      .00  .00          61.01700    .00  7.89e-10
2  br-1        -1.0     4.00  .00           79.90400    .00  1.38e-09
3  co3-2       -2.0     5.40  .00           60.00940   2.00  6.12e-10
4  ca+2         2.0     6.00  .17           40.08000    .00  5.05e-10
5  cl-1        -1.0     3.00  .01           35.45300    .00  1.33e-09
6  k+1          1.0     3.00  .01           39.10200    .00  1.31e-09
7  mg+2         2.0     6.50  .20           24.31200    .00  4.53e-10
8  na+1         1.0     4.00  .07           22.98980    .00  8.55e-10
9  so4-2       -2.0     4.00 -.04           96.06160    .00  6.83e-10
10 sr+2         2.0     5.00  .00           87.62000    .00  5.11e-10
11 end
```

Figure A.9: Database File

A.9 Database File

The database file is the file where we store the charge number (first column) for each ion followed by the Debye-Huckel constants a_i and b_i (second and third column) and then on the last three columns we store the molar mass, the alkalinity and the diffusivity in m^2/s for each ion (fig. A.9).

Appendix B

Ionic Strength - Activity Coefficients

In the theory of electrolyte solutions, an ideal solution is one whose colligative properties (properties that depend on the ratio of the number of solute particles to the number of solvent molecules in a solution) are proportional to the concentration of the solute. But this ideality differs from real solutions since, as concentrations of solutes grow, they can "screen" each other. In order to account for these effects in thermodynamics, the concept of activity was introduced. The colligative properties are then taken to be proportional to the activities of the ions where activity, a, is related to concentration, c with a proportionality constant known as an activity coefficient, γ, which itself depends on concentration (Wright, 2007).

$$a = \gamma \frac{c}{c^0} \tag{B.1}$$

where c^0 is a reference concentration of standard conditions for ideal behaviour.

In an ideal solution the activity coefficients for all the ions are equal to one. Only in very dilute solutions we can achieve the ideality of an electrolyte solution. The non-ideality of more concentrated solutions arises because ions of opposite charge will attract each other due to electrostatic forces, while ions of the same charge repel each other. The typical activity of seawater according to Millero (2001) is $\approx$0.98.

B.1 Debye-Huckel Theory

The Debye–Hückel theory is a theoretical approach proposed by Peter Debye and Erich Hückel in order to explain the differences from ideality in solutions of electrolytes. The theory assumes a simplified model of electrolyte solution but gives accurate predictions of mean activity coefficients for ions in dilute solutions (Debye, 1923).

The Debye–Hückel model for activity, which is valid to low concentrations in binary solutions is (Parkhurst et al., 1999):

$$log\gamma_i = \frac{-Az_i^2\sqrt{I}}{1+Ba_i\sqrt{I}} + b_i \tag{B.2}$$

where I is the ionic strength, A and B are constants at a given temperature, a_i and b_i are ion-specific parameters and z is the charge number of ion i. This is a function of the concentration of all ions present in that solution:

$$I = \frac{1}{2}\sum c_i z_i^2 \tag{B.3}$$

where c_i is the molar concentration of ion i in mol/L. As I gets large, the activity coefficient becomes constant.

An extension of the Debye-Huckel theory is the Davies equation (Davies and Shedlovsky, 1964) which can be used to calculate activity coefficients of electrolyte solutions at low concentrations. The final form of the equation gives the activity coefficient γ of ion i as a function of ionic strength I (Parkhurst et al., 1999):

$$log\gamma_i = -Az_i^2(\frac{\sqrt{I}}{1+\sqrt{I}} - 0.24I) \tag{B.4}$$

However, as concentration increases, the second term becomes increasingly important, so the Davies equation can be used for more concentrated solutions. However, the Davies equation typically fails when $I \rightarrow 1$ mol/L. Past this point the equation lacks the ability to give accurate activity coefficients due to its simplicity. Therefore a more sophisticated approach is needed for high concentrated solutions, typically Pitzer equations are used.

B.2 Pitzer Theory

The Pitzer equations consist of parameters which are linear combinations of parameters, of a virial expansion of the excess Gibbs free energy, which characterise interactions amongst ions and solvent (Pitzer, 1991).

The derivation of the parameters is foremost from experimental data such as the osmotic coefficient, mixed ion activity coefficients, and salt solubility. These parameters are used in order to calculate mixed ion activity coefficients and water activities in solutions of high ionic strength for which the Debye–Hückel theory is no longer adequate.

B.2.1 Pitzer Model

The Pitzer equations for the activity coefficient of a cation M (γ_M) and the activity coefficient of an anion X(γ_X) are as follows:

$$ln(\gamma_M) = z_M^2 F + \sum_a m_a(2B_{Ma} + ZC_{Ma}) + \sum_c m_c(2\Phi_{Mc} + \sum_c m_a \psi_{Mca}) + \sum_{a<a'}\sum m_a m_{a'} \psi_{Maa'} + z_M \sum_c \sum_a m_c m_a C_{Ca} \quad \text{(B.5)}$$

$$ln(\gamma_X) = z_X^2 F + \sum_c m_c(2B_{cX} + ZC_{cX}) + \sum_a m_a(2\Phi_{Xa} + \sum_c m_c \psi_{cXa}) + \sum_{c<c'}\sum m_c m_{c'} \psi_{cc'X} + z_X \sum_c \sum_a m_c m_a C_{Ca} \quad \text{(B.6)}$$

The summations in eq. B.5 and B.6 over a and c are summations over the anions and cations respectively present in the solution. The various terms used in these equations are defined as:

$$Z = \sum_i m_i \mid z_i \mid \quad \text{(B.7)}$$

$$F = f^\gamma + \sum_c \sum_a m_c m_a B'_{ca} + \sum_{c<c'}\sum m_c m_{c'} \Phi_{cc'} + \sum_{a<a'}\sum m_a m_{a'} \Phi_{aa'} \quad \text{(B.8)}$$

$$f^\gamma = A_\Phi [\frac{I^{1/2}}{1 + bI^{1/2}} + \frac{2}{b} ln(1 + bI^{1/2})] \quad \text{(B.9)}$$

Table B.1: The parameters mentioned above and their clasification as mixture dependent parameters of the Pitzer model (D) or independent (I)

Parameter	Units	D/I
Interaction parameter A_Φ	-	I
Interaction parameter B	-	I
Interaction parameter b	-	I
Interaction parameter C	-	D
Shielding parameter F	Cmol$^-$1	I
Interaction parameter f^γ	-	I
Ionic Strength I	mol kg$^-$1	I
Molecular weight M_i	kg mol$^-$1	I
Molality of component i m_i	mol kg$^-$1	I
Modified ionic strength Z	mol kg$^-$1	I
Ionic charge of component i z_i	-	I
Activity coefficient i γ_i	-	I
Interaction parameter Φ	-	I
Interaction parameter Ψ	-	D

$$I = \frac{1}{2}\sum c_i z_i^2 \tag{B.10}$$

Using the Pitzer equation the different parameters are listed in table B.1, where the parameters are classified as dependent or independent on the the model's properties.

Appendix C

Derivation of Diffusivity Equation for Binary Salt

We start from the equation for the total diffusion flux with both the diffusive and electrical potential driven fluxes.

$$J_i = -\frac{\kappa_i^0 c_i \partial \mu_i}{RT \partial c_i} \nabla c_i - \frac{\kappa_i^0 c_i F z_i}{RT} \nabla \Phi \tag{C.1}$$

Assuming electroneutrality where:

$$\sum_{i=1}^{N} z_i J_i = 0 \tag{C.2}$$

$$0 = J_1 z_1 + J_2 z_2 \tag{C.3}$$

We can get $\nabla\Phi$ to be:

$$\nabla \Phi = \frac{RT}{F} \frac{(\kappa_1 - \kappa_2)\nabla c_i}{(z_1 \kappa_1 - z_2 \kappa_2) c_i} \tag{C.4}$$

By substituting $\nabla\Phi$ in eq. B.1 we get:

$$-J_i = \frac{\kappa_1 \kappa_2 (c_1 z_1^2 + c_2 z_2^2)}{\kappa_1 c_1 z_1^2 + \kappa_2 c_2 z_2^2} \nabla C_i \tag{C.5}$$

And:

$$\kappa = \frac{\kappa_1 \kappa_2 (c_1 z_1^2 + c_2 z_2^2)}{\kappa_1 c_1 z_1^2 + \kappa_2 c_2 z_2^2} \tag{C.6}$$

Also, since we have charge balance:

$$\sum z_i c_i = 0 : c_1 z_1 + c_2 z_2 = 0 \tag{C.7}$$

So that our diffusivity for a binary salt will be:

$$\kappa = \frac{(\mid z_1 \mid + \mid z_2 \mid) * \kappa_1 \kappa_2}{\mid z_1 \mid * \kappa_1 + \mid z_2 \mid * \kappa_2} \tag{C.8}$$